RESISTANCE WELDING OF PAEK / CARBON FIBER THERMOPLASTIC COMPOSITE LAMINATES

A THESIS SUBMITTED TO
THE GRADUATE SCHOOL OF NATURAL AND APPLIED SCIENCES
OF
MIDDLE EAST TECHNICAL UNIVERSITY

BY

İSMAİL BAHA MARTI

IN PARTIAL FULFILLMENT OF THE REQUIREMENTS
FOR
THE DEGREE OF MASTER OF SCIENCE
IN
METALLURGICAL AND MATERIALS ENGINEERING

JANUARY 2023

Approval of the thesis:

RESISTANCE WELDING OF PAEK / CARBON FIBER THERMOPLASTIC COMPOSITE LAMINATES

submitted by **İSMAİL BAHA MARTI** in partial fulfillment of the requirements for the degree of **Master of Science** i**n Metallurgical and Materials Engineering, Middle East Technical University** by,

Prof. Dr. Halil Kalıpçılar
Dean, Graduate School of **Natural and Applied Sciences** _____

Prof. Dr. Ali Kalkanlı
Head of the Department, **Metallurgical and Materials Eng.** _____

Prof. Dr. Cevdet Kaynak
Supervisor, **Metallurgical and Materials Eng., METU** _____

Examining Committee Members:

Prof. Dr. C. Hakan Gür
Metallurgical and Materials Eng., METU _____

Prof. Dr. Cevdet Kaynak
Metallurgical and Materials Eng., METU _____

Prof. Dr. Bora Maviş
Mechanical Engineering, Hacettepe University _____

Assoc. Prof. Dr. Batur Ercan
Metallurgical and Materials Eng., METU _____

Assist. Prof. Dr. Çiğdem Toparlı
Metallurgical and Materials Eng., METU _____

Date: 20.01.2023

I hereby declare that all information in this document has been obtained and presented in accordance with academic rules and ethical conduct. I also declare that, as required by these rules and conduct, I have fully cited and referenced all material and results that are not original to this work.

Name Last name: İsmail Baha Martı

Signature:

ABSTRACT

RESISTANCE WELDING OF PAEK / CARBON FIBER THERMOPLASTIC COMPOSITE LAMINATES

Martı, İsmail Baha
Master of Science, Metallurgical and Materials Engineering
Supervisor: Prof. Dr. Cevdet Kaynak

January 2023, 73 pages

The main purpose of this thesis is, as the first time in the literature, to investigate usability of resistance welding joining method for poly(aryletherketone) (PAEK) thermoplastic matrix carbon fiber (CF) reinforced composite laminates (PAEK/CF).

For this purpose, effects of six different Interlayer Forms having different stainless steel meshes as Heating Elements and different woven glass fiber forms as Insulating Layers were studied. After determining welding parameters for each specimen group, performance of the resistance welding operations was compared by ultrasonic inspection, microscopic examination, DSC analyses, and by three different interlaminar mechanical tests.

Analyses and tests generally revealed that use of stainless steel meshes as Heating Elements could supply proper amperage level for the heating, melting and crystallization stages of the PAEK matrix during welding consolidation. It was also observed that in order to prevent Current Leakage problem to the other layers in the composite laminate, rather thicker and heavier woven glass fiber forms as Insulating Layers should be used. Otherwise, not only voids could form in the

thermoplastic matrix, but also delamination might occur in the upper or lower composite laminates being welded.

Keywords: Poly(aryletherketone) (PAEK), Carbon Fiber (CF), Resistance Welding, Interlayer Form, Heating Element, Insulating Layer.

ÖZ

PAEK / KARBON ELYAF THERMOPLASTİK KOMPOZİT LAMİNATLARIN DİRENÇ KAYNAĞI

Martı, İsmail Baha
Yüksek Lisans, Metalurji ve Malzeme Mühendisliği
Tez Yöneticisi: Prof. Dr. Cevdet Kaynak

Ocak 2023, 73 sayfa

Bu tezin temel amacı, literatürde ilk kez, direnç kaynağı birleştirme yönteminin poli(arileterketon) (PAEK) termoplastik matris karbon elyaf (CF) takviyeli kompozit laminatlar (PAEK/CF) için kullanılabilirliğini araştırmaktır.

Bu amaçla, Isıtma Elemanları olarak farklı paslanmaz çelik ağlara ve İzolasyon Katmanları olarak farklı dokuma cam elyaf formlarına sahip altı farklı Ara Katman Formunun etkileri incelenmiştir. Her numune grubu için kaynak parametreleri belirlendikten sonra, direnç kaynağı işlemlerinin performansı ultrasonik muayene, mikroskobik inceleme, DSC analizleri ve üç farklı tabakalar arası mekanik test ile karşılaştırıldı.

Analizler ve testler genel olarak paslanmaz çelik ağların Isıtma Elemanları olarak kullanılmasının, kaynak birleştirme sırasında PAEK matrisinin ısıtma, eritme ve kristalleşme aşamaları için uygun amper sağlayabileceğini ortaya koydu. Kompozit laminatta diğer katmanlara Akım Sızıntısı sorununun önlenmesi için Yalıtım Katmanları olarak oldukça kalın ve ağır dokunmuş cam elyaf formlarının kullanılması gerektiği de gözlenmiştir. Aksi takdirde, termoplastik matriste

boşluklar oluşabileceği gibi, kaynak yapılan üst veya alt kompozit laminatlarda da delaminasyon meydana gelebilir.

Anahtar Kelimeler: Poli(arileterketon) (PAEK), Karbon Elyaf (CF), Direnç Kaynağı, Ara Katman Formu, Isıtma Elemanı, İzolasyon Katmanı.

To my love and family

ACKNOWLEDGMENTS

First of all, I would like to convey my special thanks to my advisor Prof. Dr. Cevdet Kaynak for his endless support, guidance and efforts throughout the thesis study and my entire graduate program. I also would like to express my appreciation for his patience and understanding in the compelling time of pandemic.

I would like to express my gratitude to the examining committee, Prof. Dr. C. Hakan Gür, Prof. Dr. Bora Maviş, Assoc. Prof. Dr. Batur Ercan and Assist. Prof. Dr. Çiğdem Toparlı for their precious evaluation and recommendations during my thesis defense period of time.

I would like to state my gratefulness to Physico-Chemical and Mechanical Laboratories of Materials Engineering Department at Turkish Aerospace where all experimental analyses and tests were conducted. I also would like to express my deepest gratitude to Advanced Engineering Applications Department (Tunç Koç, Halil Nezih Sezer, İbrahim Aydoğan, Mehmet Oruç, Oğuzhan Yavuz) at Turkish Aerospace for their endless contribution, supervision and guidance in the field of practice.

I would like to state my thankfulness to my dearest parents, brother and sister for supporting, loving and believing in me throughout my entire life. I am very glad to have them at every stage of my life.

Lastly, I cannot express my true feelings and gratefulness enough for Didem Büşra Çalışkan, who always believed in me, shared my burdens and never preserved her support in every aspect of my life.

TABLE OF CONTENTS

ABSTRACT v

ÖZ vii

ACKNOWLEDGMENTS x

TABLE OF CONTENTS xi

LIST OF TABLES xiii

NOMENCLATURE xvi

CHAPTERS

1 INTRODUCTION 1

1.1 Fiber Reinforced Thermoplastic Matrix Composites 1

1.2 Resistance Welding Process 6

1.3 Process Parameters of Resistance Welding 10

1.4 Applications of Resistance Welding 12

1.5 Literature Review on Resistance Welding 13

1.6 Aim of the Thesis 17

2 EXPERIMENTAL WORK 19

2.1 PAEK/CF Thermoplastic Composite Laminates to be Welded 19

2.2 Preliminary Analyses Conducted for the PAEK/CF Laminates 22

2.3 Production of Six Different Interlayer Forms (IF) 24

2.4 Resistance Welding Operations 29

2.5 Ultrasonic Inspection and Machining of the Welded Specimens 31

2.6 Mechanical Testing of the Welded Specimens 32

3 RESULTS AND DISCUSSION 37

3.1 Preliminary Analyses of the PAEK/CF Laminates 37

3.2 Determination of the Resistance Welding Parameters for Each Interlayer Forms. 42

3.3 Ultrasonic Inspection of the Welded Specimens 44

3.4 Effects of Interlayer Forms on the Mechanical Performance of Welded Specimens 47

3.5 Interlaminar Failure Modes Observed During Testing of Welded Specimens 53

3.6 Microscopic Analyses of the Welded Specimens 58

3.7 DSC Analyses of the Welded Specimens 60

3.8 Comparison of the Welding Performance with Other Studies 62

4 CONCLUSIONS 65

REFERENCES 69

LIST OF TABLES

TABLES

Table 2.1 Thermal and certain other properties of PAEK thermoplastic matrix given by the supplier. 20

Table 2.2 Details of the lower and upper PAEK/CF laminates to be welded..... 20

Table 2.3 Mechanical properties of the lower and upper PAEK/CF laminates given by the supplier..... 21

Table 2.4 Properties of the two different heating elements used..... 25

Table 2.5 Properties of the three different insulating layers used. 26

Table 2.6 Six different lay-up configurations used in the Interlayer Forms..... 27

Table 3.1 Results of the three preliminary analyses conducted for the upper and lower PAEK/CF laminates before welding. Note that the last column in the table gives the suppliers data for comparison. 41

Table 3.2 Optimum amperage parameters determined for the resistance welding operations of Six different Interlayer Forms. 43

Table 3.3 Average values of the interlaminar fracture toughness (G_{IC}, G_{IIC}) and interlaminar shear strength (SLSS) values of the welded specimens with six different Interlayer Forms. 52

Table 3.4 Average Thickness Deviation and Porosity Level after welding of the specimens with six different interlayer forms. 59

Table 3.5 Glass Transition Temperature (T_g) range and Crystallinity Degree (Xc) of the PAEK matrix of welded specimens with six different interlayer forms. 60

Table 3.6 Comparison of the mechanical properties obtained in the resistance welding of this study for PAEK/CF laminates with IF-1 interlayer form and the other studies conducted for PEEK/CF and PEI/CF laminates. 63

LIST OF FIGURES

FIGURES

Figure 1.1 Monomer structure of (a) PEEK, (b) PEKK, (c) PAEK, (d) PPS. 2
Figure 1.2 Examples of continuous fiber forms; (a) Unidirectional, (b) Plain weave, (c) 8-Harness satin weave. 3
Figure 1.3 Typical laboratory-scale resistance welding set-up [3]. 6
Figure 1.4 Typical structure of the Interlayer Form having (i) Heating element, (ii) Neat thermoplastic film, (iii) Insulating layer. 7
Figure 1.5 Resistance welding of ribs to the leading edge of a passenger airplane [7]. 12
Figure 2.1 Cutting of large plates (left) into lower and upper strips (right) for welding. 21
Figure 2.2 Composition of the sublayers in the Interlayer Form used. 24
Figure 2.3 Steps during consolidation of the interlayer forms; (a) A plate of IF lay-up's on a tool, (b) Plastic bagging of the IF plate, (c) Consolidation in the autoclave, (d) IF plates after consolidation, (e) IF plate after demolding, and (f) IF strips after cutting. 28
Figure 2.4 Typical Temperature - Time profile during four thermal stages required in resistance welding of the thermoplastic matrix composite laminates. Note that, values given in the axes are typical ranges for the PAEK matrix. 30
Figure 2.5 Machining operation (above) and mechanical test specimen examples after machining (below). 31
Figure 2.6 Specimen geometry (above) and Mode-I loading fixture (below) of the G_{IC} tests. 33
Figure 2.7 Specimen geometry (above) and Mode-II loading fixture (below) of the G_{IIC} tests. 34
Figure 2.8 Specimen geometry (above) and tensile loading fixture (below) of the SLSS tests. 36

Figure 3.1 Example of the through-thickness optical microscope image analysis for the upper and lower PAEK/CF laminates. 39
Figure 3.2 Example of the first heating DSC thermograms for the upper and lower PAEK/CF laminates. 40
Figure 3.3 Example of the temperature-time profile obtained from three different thermocouples for the IF-1 Interlayer Form. 43
Figure 3.4 C-scan images obtained from the AUTT inspection of the four welded strips for each IF-1, IF-2 and IF-3 Interlayer Forms. 45
Figure 3.5 C-scan images obtained from the AUTT inspection of the four welded strips for each IF-4, IF-5 and IF-6 Interlayer Forms. 46
Figure 3.6 Load vs. displacement curves obtained during G_{IC}, G_{IIC} and SLSS tests. 50
Figure 3.7 Effects of Interlayer Forms on the interlaminar fracture toughness (G_{IC}, G_{IIC}) and shear strength (SLSS) values of the welded specimens. 51
Figure 3.8 Four typical interlaminar failure modes; (i) cohesive, (ii) adhesive, (iii) delamination and (iv) mixed failure that might be observed during the mechanical tests of welded specimens. 53
Figure 3.9 Examples of interlaminar failure modes observed during G_{IC} tests. From top to down: Cohesive, adhesive, mixed (cohesive and delamination). 55
Figure 3.10 Examples of interlaminar failure modes observed during G_{IIC} tests. From top to down: Cohesive, adhesive, delamination. 56
Figure 3.11 Examples of interlaminar failure modes observed during SLSS tests. From top to down: Cohesive, adhesive, mixed (cohesive and delamination). 57
Figure 3.12 One example of the through-thickness optical microscope image analysis conducted after welding. 59
Figure 3.13 Examples of the first heating DSC thermograms of the welded specimens with six different Interlayer Forms. 61

NOMENCLATURE

ABBREVIATIONS

ASTM	American Society for Testing and Materials
CF	Carbon Fiber
DSC	Differential Scanning Calorimetry
EN	European Technical Standards
GF	Glass Fiber
GSM	Gram per Square Meter
G_{IC}	Interlaminar Fracture Toughness Mode-I
G_{IIC}	Interlaminar Fracture Toughness Mode-II
HE	Heating Element
MUPE	Manual Ultrasonic Pulse-Echo
MWCNT	Multi-Wall Carbon Nanotubes
NDI	Non-Destructive Inspection
PAEK	Poly(aryletherketone)
PEEK	Poly(etheretherketone)
PEI	Poly(etherimide)
PI	Polyimide
PEKK	Poly(etherketoneketone)
PPS	Poly(phenylenesulfide)
RC	Resin Content
SLSS	Single Lap Shear Strength

T_g	Glass-transition Temperature
T_m	Melting Temperature
TTU	Thru-Transmission Ultrasonic
UD	Unidirectional
W	Woven
ρ	Density
5HS	Five Harness-Satin

CHAPTER 1

INTRODUCTION

Fiber reinforced polymer matrix composites have been used for decades in many industries such as aerospace, automotive, maritime, sports and so on. For these structural applications, the matrix material used were especially thermoset polymer resins including epoxies, polyesters and phenolics. Although these composites are still being used for many purposes; they have certain shortcomings such as insufficient toughness, low strain to failure, very limited shelf life of the resins, extremely long and rigid multi-step processing techniques [1]. Therefore, in order to overcome these deficiencies of thermoset matrices, both academia and industry are exploring and developing fiber reinforced structural composites with thermoplastic matrices.

1.1 Fiber Reinforced Thermoplastic Matrix Composites

These structural composite materials could be overviewed in terms of their matrix materials, fiber types and forms, prepregs and laminates, and their joining techniques.

(i) *Thermoplastic Matrices Used*

Although many engineering thermoplastics could be used as the matrix material for a variety of applications, aerospace industry especially prefers higher mechanical performance, higher temperature resistant, semi-crystalline engineering thermoplastics such as poly(etheretherketone) (PEEK), poly(etherketoneketone) (PEKK), poly(aryletherketone) (PAEK) and poly(phenylenesulfide) (PPS). Due to their semi-crystalline structure and aromatic groups present in their monomers

(Figure 1.1), it is possible to use them even above their glass transition temperatures. In this study, thermoplastic composite laminates to be welded has PAEK matrix.

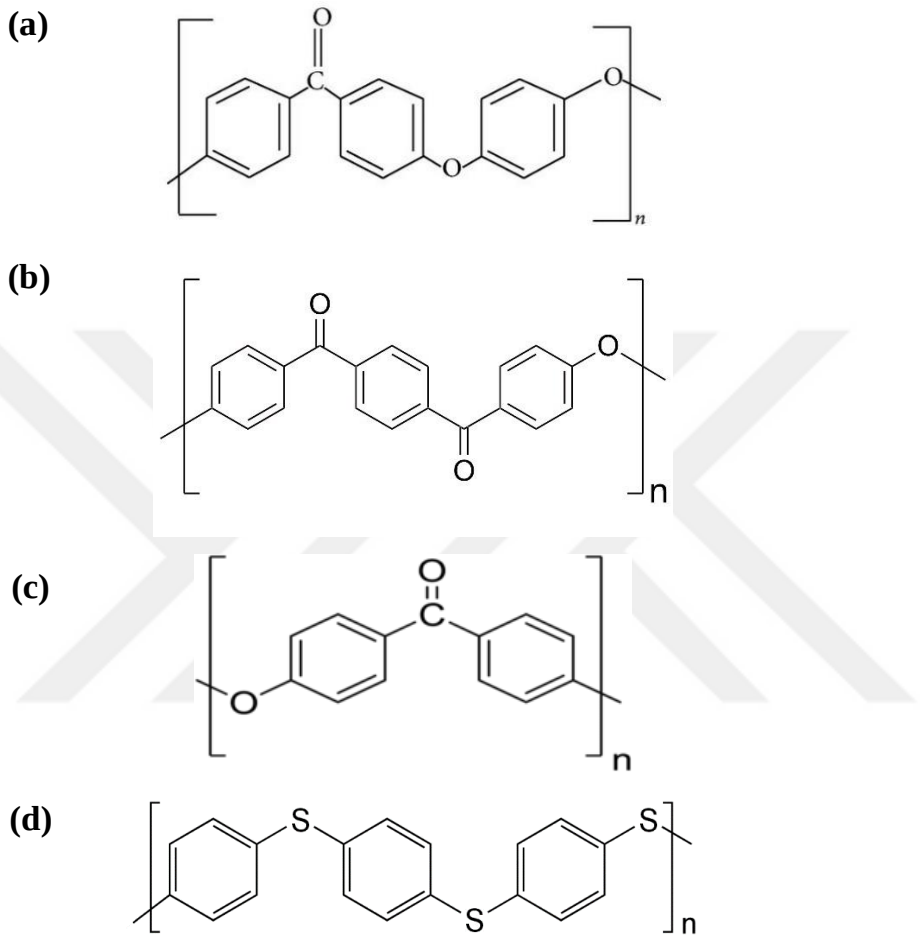

Figure 1.1 Monomer structure of (a) PEEK, (b) PEKK, (c) PAEK, (d) PPS.

(ii) ***Fibers and Their Forms Used***

Although various particles and short fibers could be used as the reinforcement material for many applications, structural parts in aerospace industry require "continuous fibers". Just like in the traditional thermoset matrix composites, "glass, carbon, aramid" continuous fibers are also preferred in the thermoplastic matrix composites.

Depending on the loading conditions of the laminate structure, and the processing techniques used; continuous fibers could be used in different forms, mainly as "unidirectional" form or "woven" form. There are various "weave styles" available in the market, the most widely used ones being "plain weave" and "satin weave" with various configurations such as 5-harness satin or 8-harness satin, etc. (Figure 1.2).

In this study, welding operations were conducted between the PAEK matrix composite laminates; the lower one having unidirectional (UD) form and the upper one having 5-harness satin (5HS) woven forms of continuous carbon fibers (CF).

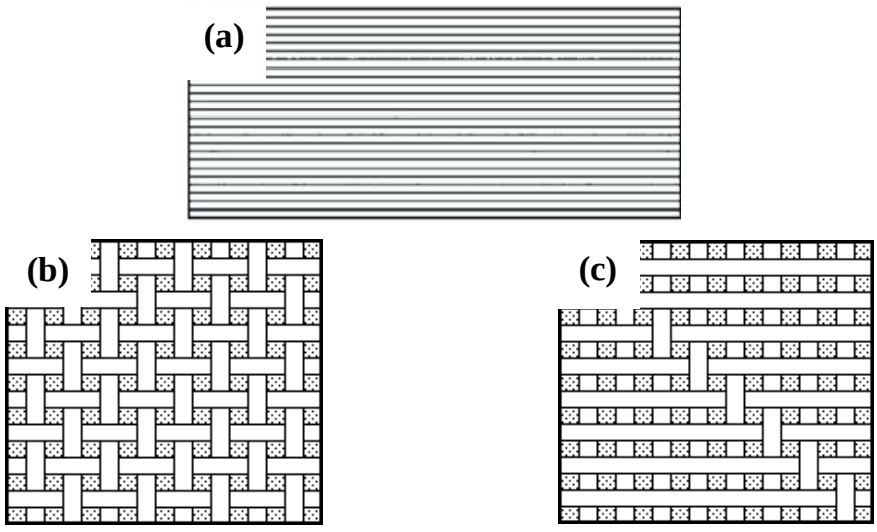

Figure 1.2 Examples of continuous fiber forms; (a) Unidirectional, (b) Plain weave, (c) 8-Harness satin weave.

(iii) *Prepregs and Consolidated Laminates*

It is known that impregnation of the continuous fiber forms with polymer matrix resins is rather a time-consuming problematic issue for the end user. Therefore, just like traditional thermoset resin pre-impregnated fiber forms, i.e. “pre-pregs”; it is also possible, especially for aerospace industry, to supply very practical “thermoplastic pre-preg forms”. Moreover, apart from supplying these thermoplastic pre-preg forms as “single layers”, today it is also possible to get them in the form of “consolidated laminates” having certain number of pre-preg layers with certain thicknesses.

In this study, the lower laminate to be welded consists of 24 layers of unidirectional PAEK/CF pre-pregs while the upper laminate is comprised of 8 layers of 5-harness satin woven PAEK/CF pre-pregs.

(iv) *Joining Techniques of Thermoplastic Matrix Composites*

Although there are well established mechanical fastening and adhesive bonding techniques for the traditional thermoset matrix composite structures, they are not directly applicable to the continuous fiber reinforced thermoplastic composite structures. In aerospace industry, the most common four methods utilized to join thermoplastic matrix composite structures are as follows:

- **Co-Consolidation:** In this method, no interlayers are used. Two pieces having compatible thermoplastic matrices are compressed under heat. Joining takes place via intertwining of the macromolecular chains of the matrices during consolidation.

- **Resistance Welding:** This technique uses a specific “Interlayer Form” having a heating medium in between the two composite parts to be joined. When current passes through the heating medium, sufficient level of energy

develops to join the compatible thermoplastic matrices via chain intertwining mechanism.

- **Induction Welding:** In this technique, intertwining of the thermoplastic chains could form via an induction coil used to produce the eddy current on the surface of one of the composite parts to be welded.

- **Ultrasonic Welding:** In this technique, ultrasonic vibrations produced via a sonotrode powered by an electric generator are used to heat the surfaces of the composite parts, so that vibrational energy would lead to intertwining between the two thermoplastic matrices.

In this study, since “Resistance Welding” is the main technique used in aerospace industry; effects of certain parameters on the performance of this welding method for PAEK/CF thermoplastic matrix composite laminates are investigated.

1.2 Resistance Welding Process

The resistance welding process, also called as resistive implant welding or electro-fusion, basically includes placing an interlayer form having conductive heating element between the composite laminates to be welded. Electrical current generated by power supply unit is circulated across the weld-line to rise the temperature at the interface [2]. According to the Joule's Law, the energy emitted from the resistor is proportional to the resistance, current and elapsed time:

$$E = I^2 R\ x\ t$$

Heat affected zone in the process has to be as close to the joining surfaces as possible in order to avoid porosity, delamination, fiber disturbance and so on. The temperature of the joining surfaces should be above T_g for amorphous and T_m for semi-crystalline thermoplastic matrices. After that, the current is reduced to a very low degree to cool down the materials under applied constant pressure.

Figure 1.3 indicates a typical laboratory-scale resistance welding set-up showing main parts of the system, as discussed one by one below:

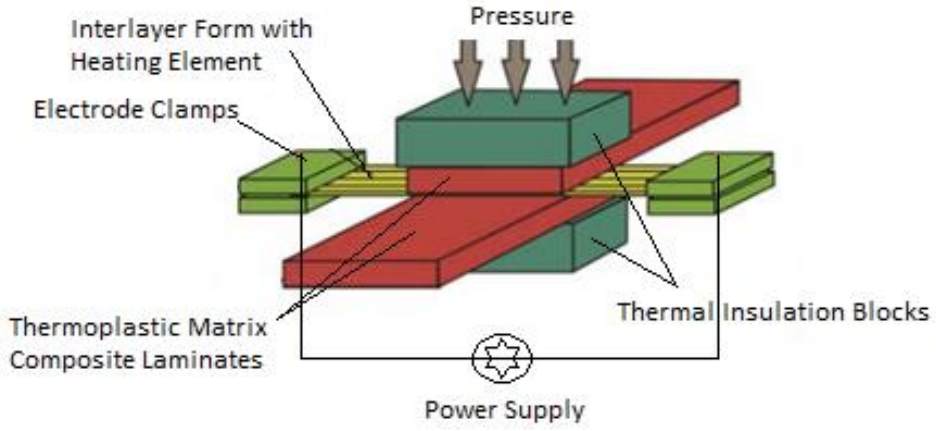

Figure 1.3 Typical laboratory-scale resistance welding set-up [3].

(i) *Thermoplastic Matrix Composite Laminates*

Resistance welding technique could be used for joining of various thermoplastic matrix composite laminates. In this study, PAEK matrix with continuous UD and woven 5HS carbon fiber laminates are studied.

(ii) *Interlayer Form with Heating Element*

One of the most significant piece in resistance welding operations is the "Interlayer Form" placed in between the two composite parts to be joined (Figure 1.4).

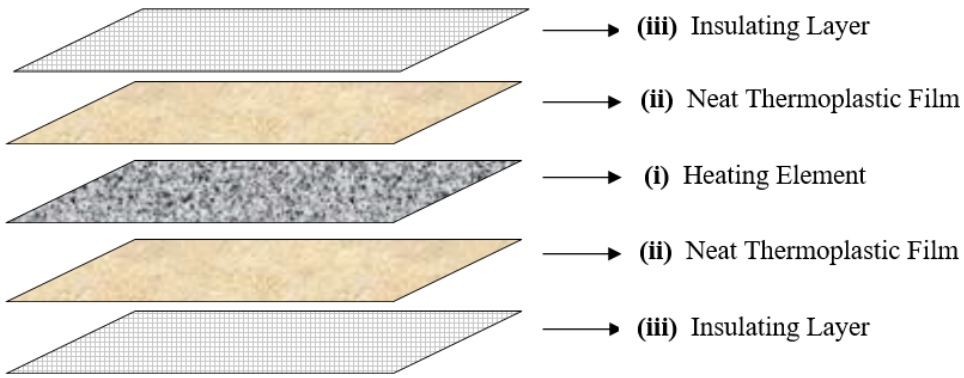

Figure 1.4 Typical structure of the Interlayer Form having (i) Heating element, (ii) Neat thermoplastic film, (iii) Insulating layer.

The main layer located in the center of this form is named as conductive "Heating Element". When power supply unit gives electric current to the heating element, it melts the surrounding thermoplastic matrix of the composite laminates. Heating element cannot be taken out from the interface, it remains within the composite joint.

Although there are other conductive materials available, the most widely used heating element in the industry is the various forms of "stainless steel meshes" because stainless-steel mesh forms give uniform current distribution across the weld, which prevents possible anomalies in the temperature profiles and formation

of flaws in the weld. In this study, use of two different stainless-steel mesh forms is investigated.

Interlayer forms might have only heating element layers; on the other hand, to achieve higher performance in resistance welding operations, interlayer forms might also include two more very thin layers located above and below the heating element central layer as shown in Figure 1.4.

The function of the "Neat Thermoplastic Film" is to increase the resin content in between the heating element and insulating layer for a better joining performance. It is usually chosen as the thin film layer made of the same thermoplastic matrix used in the composite laminates to be welded. Thus, in this study, thin films of PAEK were used.

The function of the "Insulating Layer" is to insulate other layers of the laminate from the welding current so that they might be kept away from any thermal damages. This layer used in the industry is usually woven forms of Glass Fibers (GF) impregnated with the same thermoplastic matrix as the laminates. Thus, in this study, effects of three insulating layers having PAEK impregnated three different GF forms were evaluated.

(iii) ***Thermal Insulation Blocks***

The function of the thermal insulation blocks in the resistance welding system is to avoid temperature outflow causing heat loss in the system. Researchers investigated effects of different thermal insulation blocks of maronite, ceramic, oak wood, silicon rubber, high-density fibre wood, asbestos, etc. [4].

(iv) ***Electrode Clamps and Thermocouples***

Electrode clamps made of metals with excellent conductivity are used to obtain maximum conductance in the heating element for consistent weld-line. For this purpose, certain level of pressure is also applied to the clamps.

Before the start of welding operation, thermocouples are used to monitor the level and distribution of the temperature in the welding zone. After control, thermocouples must be taken out from the interface.

(v) ***Pressure Unit and Power Supply***

Pressure being a significant parameter during resistance welding operations can be applied by a pneumatic press to provide homogenous pressure distribution on the surfaces of the composite parts to be joined.

Power unit as the voltage supplier can deliver either direct or alternating current as both are applicable and feasible in the welding process. Capacity of power supply unit is significant in resistance welding operations since the voltage and the amperage values obtained from the unit must be sufficient for the sizes of the composite parts to be joined.

1.3 Process Parameters of Resistance Welding

Consolidation is one of the most crucial step during all manufacturing processes of continuous fiber reinforced thermoplastic matrix composite parts. It is simply hot pressing of matrix and fiber layers or their prepregs to achieve proper interlayer adhesion and to get a consistent thickness for the composite laminate structure. Of course, for the semi-crystalline thermoplastic matrices, proper cooling parameters are also required in order to achieve higher degree of matrix crystallinity. Therefore, "consolidation" is also significant during resistance welding operation. There are four main process parameters of resistance welding process influencing the consolidation level and degree of crystallinity of the thermoplastic matrix of the composite parts to be welded.

(i) *Power Level*

Power level is one of the key parameters of resistance welding process since the voltage and amperage levels determine the resistance level of the heating element and the other components of the system. Therefore; depending on the size of the welded structure, level of the power should be sufficient to achieve desired processing temperature within the desired time interval.

(ii) *Pressure Level*

Pressure level is also an essential parameter of resistance welding process since it should enable the intimate contact of the composite laminates at the interface, so that intertwining of the macromolecular chains required between the matrices of the two laminates being welded could be achieved.

(iii) *Melting Dwell Time*

During resistance welding, the temperature of the interface should be over the melting point of the thermoplastic matrix. After reaching this temperature, a sufficient period will be required to get homogenous melting throughout the interface. That period is called as “dwell time” or hold time. It is determined according to the applied power level and the resistance value of the heating element. As the power level increases, the dwell time decreases. It is significant that melting dwell time should be determined properly in order to prevent “thermal degradation” possibility of molten thermoplastic matrices during welding.

(iv) *Crystallization Dwell Time*

After elapsing the required melting dwell time during resistance welding, the cooling phase under pressure begins. During this step, crystallization of the thermoplastic matrix starts. Depending on the “crystallization degree” of the semi-crystalline thermoplastic matrix, a sufficient time interval would be required, which is called as “Crystallization Dwell Time”. Since, crystalline regions in the structure of the thermoplastic matrices improve mechanical performance of the laminates, it is important to determine the optimum value of that dwell time.

1.4 Applications of Resistance Welding

In the last two decades, use of high temperature resistant thermoplastic matrices reinforced with high mechanical performance continuous fibers are increasing especially in aerospace industry such as aircrafts, UAVs, helicopters, drones, satellites, etc. Therefore, use of resistance welding process for joining of the components in these structures became inevitable. Common examples for the resistance welded parts are stiffeners, ribs, spars, wedges and stringers to primary load carrier parts such as composite skins of fuselages, spoilers, landing doors, ailerons, etc. [5].

Figure 1.5 shows an example of the large-scale resistance welding process used in the joining of glass fiber reinforced PPS ribs to the leading edges of a commercial passenger airplane [6, 7].



Figure 1.5 Resistance welding of ribs to the leading edge of a passenger airplane [7].

1.5 Literature Review on Resistance Welding

Literature review revealed that although there are extensive number of studies [8-27] on the ultrasonic welding and induction welding, the number of the studies on resistance welding are rather limited [28-37]; being especially on the heat transfer modelling of parameters and effects of interlayer form, as summarized below.

(i) *Studies on the Modelling of Process Parameters*

Ageorges *et al.* [28] used both thermal imaging and three-dimensional heat transfer modelling to determine the process parameters for welding of carbon fiber reinforced polyetherimide (PEI) composite laminates. As the heating element of the process, unidirectional and woven carbon fiber forms were utilized while for the insulating layer glass fiber forms impregnated with PEI were used. Joining performance of the interface was evaluated by applying lap shear strength and double-cantilever beam tests. As a result of the study, it is found that the temperature distribution through the woven heating element was more homogenous, and the temperature distribution predictions obtained via finite-element model was slightly higher than the recorded values during the welding operations.

In the study of Xiao *et al.* [29], thermal analysis by using two-dimensional finite element modelling was used to select the process parameters for welding of carbon fiber reinforced PEEK composite laminates. Heating element selected was also carbon fiber forms. Evaluations on the mechanical performance of the joint was made by applying single lap shear strength tests and examining the microstructure of the weld-line. They indicated that when the optimum parameters determined were used, 34 MPa lap shear strength could be obtained.

Jakobsen *et al.* [30] conducted a study on transient two-dimensional thermal model for resistance welding of carbon fiber reinforced PEEK composite laminates to

determine the optimum processing parameters. A single layer of unidirectional carbon fiber form was used as the heating element along with two neat PEEK films wrapping around the heating element to avoid current leakage from the interface. Double cantilever beam specimens were tested to evaluate the mechanical performance of the joints in terms of Mode-I fracture toughness values. They revealed that when the optimum welding parameters determined by the model were used; fracture toughness value of the welded laminate (2 kJ/m^2) would be almost the same obtained from the compression molded (without welding) laminate, i.e. almost 100% match.

Colak *et al.* [31] investigated the resistance welding of carbon fiber reinforced PEEK composite laminates with varying thicknesses by using one-dimensional transient heat transfer model, degradation kinetics model and bonding model. Heating element used in the models were also carbon fiber forms. They indicated that the optimum process parameters for welding of the laminates with varying thicknesses could be obtained to minimize processing time significantly without sacrificing the quality requirements such as degree of crystallinity of the PEEK matrix.

Holmes and Gillespie [32] conducted a parametric study on the usability of resistance welding for very large-scale joints of carbon fiber reinforced PEEK composite structures by using certain thermal analysis based on carbon fiber heating element forms. They indicated that process parameters especially power level could be modeled via a three-dimensional analysis to achieve sequential resistance welding of the large-scale components.

(ii) ***Studies on the Effects of Interlayer Form***

As discussed before, during resistance welding of thermoplastic matrix composite laminates, "Interlayer Form" placed between the laminates has a crucial function. It is basically composed of three layers; a heating element in the center, and very thin neat thermoplastic film and insulating layer above and below the heating element. These layers and their configurations influence the process parameters and the joint performance, significantly.

Hou and Friedrich [33] investigated effects of using carbon fiber forms as the heating element layer during resistance welding of PPS/CF composite laminates. Weld-line quality was assessed by applying lap shear strength and double cantilever beam tests. The morphology and microstructure of the contact surfaces were also analyzed by using scanning electron microscopy (SEM). They indicated that sufficient level of weld quality could be obtained within the power range of 40 to 140 kWm^{-2}. It was also observed that the intralaminar fracture toughness values were found equivalent to the ones obtained from compression molded specimens.

Hou *et al.* [34] conducted a study regarding the resistance welding of carbon fiber reinforced PEI composite laminates. They used steel meshes as the heating element to achieve uniform temperature distribution at the interface. They also used glass fiber forms impregnated with PEI to insulate the surfaces of the composite laminates from electrical current leakage. Welding parameters such as power level, welding time and pressure were optimized by using the results of microstructure analysis and mechanical tests of lap-shear strength and Mode-I fracture toughness. They revealed that power level (kW/m^2) plays a very significant role in the mechanical performance of the joints.

Howie *et al.* [35] investigated optimum parameters for the resistance welding of carbon fiber reinforced polyarylsulfone/polysulfone dual-polymer composite laminates. A single layer of carbon fiber form was used as the heating element, and both surfaces were impregnated with neat polysulfone to increase the contact

performance. Ultrasonic images and photomicrographs were used to observe the weld line, and their performance were compared with lap shear strength tests. They concluded that the bond line thickness is mainly a function of pressure and temperature rather than the welding time.

Optimum welding process parameters for carbon fiber reinforced PEEK composite laminates were also studied by Don *et al.* [36]. A single layer of unidirectional carbon fiber form was used as the heating element impregnated with neat PEEK and PEI films. In order to assess different configurations of composite laminates having unidirectional and quasi-isotropic lay-up, lap shear strength and Mode-I fracture toughness tests were conducted. Shear strength results (10-30 MPa) and fracture toughness results (0.41-1.34 kJ/m^2) were evaluated with respect to the power level, pressure level and laminate lay-up sequence; concluding that welding performance was very promising compared to the compression molded laminates without welding.

Brassard *et al.* [37] proposed an alternative heating element as 10 wt% multi-walled carbon nanotube (MWCNT) mixed into PEI matrix to be used in the resistance welding of PEEK/CF composite laminates. In order to evaluate mechanical performance of the joints, single lap shear strength tests were conducted. It was observed that due to the deficiency of uniform distribution of nanoparticles in the matrix; a non-uniform heating occurred at the weld area, resulting in rather a low shear strength of 19.6 MPa with a cohesive failure within the heating element layer. They concluded that nanocomposite approach for the heating element layer need further investigations in terms of uniform nanoparticle distribution.

1.6 Aim of the Thesis

Literature survey revealed that although there are certain number of resistance welding studies on the Carbon Fiber (CF) reinforced composite laminates having thermoplastic matrices of poly(etheretherketone) (PEEK), poly(etherimide) (PEI) and poly(phenylenesulfide) (PPS), no studies were reported on the poly(aryletherketone) (PAEK) matrix.

Therefore, the main purpose of this thesis is, as the first time in the literature, to investigate usability of resistance welding joining method for PAEK/CF thermoplastic composite laminates.

For this purpose, effects of six different Interlayer Forms having different stainless steel meshes as Heating Elements and different woven glass fiber layers as Insulating Layers were studied. After determining welding parameters for each specimen group, performance of the resistance welding operations was compared by ultrasonic inspection, microscopic examination, DSC analyses, and by three different interlaminar mechanical tests.

CHAPTER 2

EXPERIMENTAL WORK

Experimental procedures used in this study could be grouped into four main steps; (i) preparation of the thermoplastic matrix composite laminates to be welded, (ii) production of the six different interlayer form configurations, (iii) resistance welding operations, and (iv) testing and analyses for the evaluation of the weld performance.

2.1 PAEK/CF Thermoplastic Composite Laminates to be Welded

In this study, poly(aryletherketone), PAEK was selected as the matrix material for the composite laminates to be welded. Due to its lower melting point compared to other grades, it is also called as low-melt PAEK (LM-PAEK). Thermal and certain other properties of this PAEK grade given by the supplier (*Toray Advanced Materials Inc.)* are tabulated in Table 2.1.

PAEK matrix laminates reinforced with continuous carbon fiber (CF) layers were also supplied from *Toray Inc.* Two different laminates (lower and upper) used were designated as PAEK/CF-UD and PAEK/CF-W because lower laminate has unidirectional (UD) while upper laminate has 5-harness satin woven (W) fiber forms, respectively. Details of these two laminates are given in Table 2.2 while their properties given by the supplier are tabulated in Table 2.3.

Table 2.1 Thermal and certain other properties of PAEK thermoplastic matrix given by the supplier.

Properties	**Unit**	**Value**
Glass Transition Temperature Range	°C	125 - 175
Melting Temperature Range	°C	225-330
Crystallinity Onset Temperature	°C	263
Cold Crystallinity Temperature Range	°C	160 - 215
Crystallinity Degree	%	17-30
Density	g/cm^3	1.30
Shelf and Work Life	days	Indefinite at ambient temperature storage

Table 2.2 Details of the lower and upper PAEK/CF laminates to be welded.

Properties	**PAEK/CF-UD**	**PAEK/CF-W**
Matrix Resin Content	34 wt%	42 wt%
Carbon Fiber Type	T700	T300JB
Fiber Orientation	Unidirectional	5-Harness Satin
Fiber Content	58 ± 3 vol%	52 ± 3 vol%
Number of Plies	24	8
Laminate Density	1.55 ± 0.05 g/cm^3	1.55 ± 0.05 g/cm^3
Laminate Thickness	3.1 mm	2.4 mm
Photographic Image	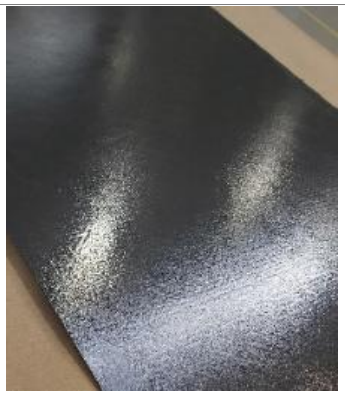	

Table 2.3 Mechanical properties of the lower and upper PAEK/CF laminates given by the supplier.

Properties	**ASTM Standard**	**Unit**	**PAEK/CF-UD**	**PAEK/CF-W**
Tensile Strength (0°)	D3039	MPa	2410	805
Tensile Modulus (0°)	D3039	GPa	135	58
Tensile Strength (90°)	D3039	MPa	86	739
Tensile Modulus (90°)	D3039	GPa	10	59
In-Plane Shear Strength	D3518	MPa	152	-
In-Plane Shear Modulus	D3518	GPa	4.3	-
Compression Strength (0°)	D664	MPa	1300	628
Compression Modulus (0°)	D664	GPa	124	52
Compression Strength (90°)	D6641	MPa	-	676
Compression Modulus (90°)	D6641	GPa	-	53
Mode I Fracture Toughness	D5528	kJ/m^2	2.1	2.25
Mode II Fracture Toughness	D7905	kJ/m^2	2.6	-

Before welding, large plates of PAEK/CF-UD and PAEK/CF-W composite laminates were cut into strips of 560 x 30 mm by using a diamond tip industrial cutter (Diamond-3, 3515RS) with a cooling unit (Figure 2.1).



Figure 2.1 Cutting of large plates (left) into lower and upper strips (right) for welding.

2.2 Preliminary Analyses Conducted for the PAEK/CF Laminates

In order to verify certain properties of the PAEK/CF laminates given by the supplier, three analyses were conducted; the first one was Fiber Volume Content determination while the others were Microstructural and Thermal Analyses.

(i) *Fiber Volume Content (FVC) Analysis*

It is known that amount of the reinforcing fibers in the composite laminates is the most crucial parameter in improving all mechanical and other properties. Therefore, in this study, ASTM D3171 [38] standard was used to determine the fiber content of the PAEK/CF laminates with sulfuric acid and hydrogen peroxide solution digestion method by using the Procedure B in the standard. First, specimens were weighted using a precision balance before holding them in the acid solution until no PAEK matrix was left. The remaining carbon fibers were washed, dried, and weighted precisely to determine their weight percentage values. Eight specimens were tested in total, with the dimensions of 20 mm x 10 mm having 3.1 mm and 2.4 mm thickness values. By using the following relation, the weight percentage of carbon fibers were transformed into volume percentages:

$$V_r = \left(M_f \,/\, M_i\right) \times 100 \times \left(\rho_c \,/\, \rho_r\right)$$

Where V_r is the reinforcement volume percent, M_i and M_f are the initial and the final mass of the specimen in grams while ρ_r and ρ_c are the density of reinforcement and the specimen in g/cm^3, respectively.

(ii) ***Microstructural Analysis***

In order to examine possible interfacial defects including porosity and fiber distortion in the PAEK/CF laminates, microstructural analyses were conducted by using *Olympus GX53* optic microscope system with an image analysis software. At least 3 measurements were conducted for each condition.

It should be noted that microstructural analyses were conducted also after the welding operations in order to reveal possible microstructural changes, especially the degree of deviations in the thickness of the welded laminates, by using the following relation:

$$x = \left(\frac{t_M}{t_N} - 1\right) \times 100$$

Where x is the thickness deviation (±%) while t_M and t_N are the measured and nominal thickness values (mm), respectively.

(iii) ***Differential Scanning Calorimetry (DSC) Analysis***

Differential scanning calorimetry (DSC) (*TA Instruments, Q100*) analyses were carried out to determine the glass transition temperature (T_g) and enthalpies of melting and cold crystallization of the PAEK matrix of the laminates under first heating profile from room temperature to 350°C at a rate of 10°C/min under nitrogen flow. At least three measurements were conducted for each condition. Degree of crystallinity of PAEK matrix was calculated by using the following relation:

$$X_c = \frac{\Delta H_m - \Delta H_{cc}}{w_{PAEK}\ \Delta H^\circ_m} \times 100$$

Where X_c is the percent crystallinity, ΔH_m is the enthalpy of melting, ΔH_{cc} is the enthalpy of cold crystallization, w_{PAEK} is the weight fraction of the PAEK matrix, and ΔH°_m is the melting enthalpy of 100% crystalline PAEK suggested by the laminate supplier as 130 J/g.

Apart from the T_g and X_c verification of the supplied PAEK/CF laminates; it should be noted that DSC analyses were conducted also after the welding operations in order to reveal whether there is any significant change in X_c values of the PAEK matrix after welding. For this purpose, very special attention was taken during the sample extraction from the welded interface.

2.3 Production of Six Different Interlayer Forms (IF)

As shown in Figure 2.2, interlayer forms used are comprised of three sublayers; (i) heating element, (ii) insulating layer and (iii) neat thermoplastic film. In this study, effects of Interlayer Form (IF) on the performance of resistance welding were investigated by constructing six different configurations. For this purpose, as the heating element layer two different stainless steel (SS) mesh forms are used while for the insulating layer three different glass fiber (GF) forms impregnated with the matrix resin are used. As the neat thermoplastic film, only one type of the neat PAEK film was used. Details of these layers are summarized below.

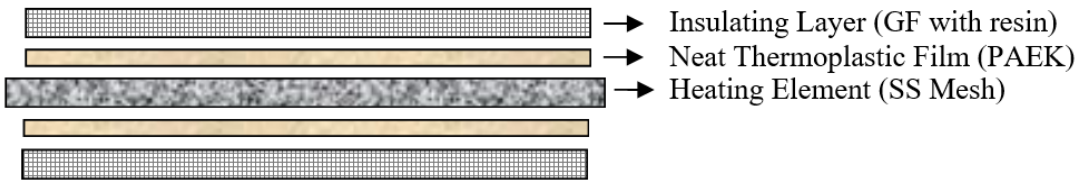

Figure 2.2 Composition of the sublayers in the Interlayer Form used.

(i) *Heating Element (HE)*

Stainless-steel meshes supplied from *Dexmet Corporation* were used as the heating element of the interlayer form to melt the matrix at the interface via electrical current. Two different heating elements used were designated as HE-1 and HE-2; having different mesh orientations, areal weights, and resistivities as tabulated in Table 2.4.

Table 2.4 Properties of the two different heating elements used.

Properties	**HE-1**	**HE-2**
Material	Stainless Steel Mesh	Stainless Steel Mesh
Areal Weight	955 gsm	479 gsm
Mesh Style	Twill 2/2	Woven Square
Resistance	0.26 Ω	0.86 Ω
Photographic Image		

(ii) *Insulating Layer (IG)*

Glass fiber (GF) woven forms impregnated with the matrix resin supplied from *Toray Inc.* were used as the electrical insulating layers to prevent current leakage to the other layers in the laminates. Three different insulating layers used were designated as IG-1, IG-2 and IG-3. As tabulated in Table 2.5, these GF layers have different matrix resin contents, different weave styles and areal weights.

Table 2.5 Properties of the three different insulating layers used.

Properties	**IG-1**	**IG-2**	**IG-3**
Matrix Resin Content	34 wt%	50 wt%	60 wt%
Glass Fiber Type	EC6 E-glass	EC5 E-glass	EC5 E-glass
Fiber Diameter	6 μm	5 μm	5 μm
Fiber Weave Style	8 Harness-Satin	4 Harness-Satin	Plain
Fiber Areal Weight	296 gsm	105 gsm	48 gsm
Photographic Image			

(iii) ***Neat Thermoplastic Film (TPF)***

The same thermoplastic type (PAEK) with the matrices of the composite laminates was used as the neat thermoplastic film (TPF) with a thickness of 60 μm. Its function was to increase the matrix resin content at the interface between the insulating layers and heating elements.

Thus, Table 2.6 shows six different Interlayer Forms used during welding operations. Note that, each form has different lay-up configuration.

Table 2.6 Six different lay-up configurations used in the Interlayer Forms.

Interlayer Forms	Lay-Up Configurations
IF-1	IG1 / TPF / HE1 / TPF / IG1
IF-2	IG2 / TPF / HE1 / TPF / IG2
IF-3	IG3 / TPF / HE1 / TPF / IG3
IF-4	IG1 / TPF / HE2 / TPF / IG1
IF-5	IG2 / TPF / HE2 / TPF / IG2
IF-6	IG3 / TPF / HE2 / TPF / IG3

Consolidation of the Interlayer Forms:

Before welding operations, these interlayer forms having many sub-layers should be converted into "one piece" form, i.e. a kind of "consolidation" process would be necessary. As shown in Figure 2.3 (a), six different lay-up configurations were constructed on a tool in the form of large plates. Then, these plates were covered with a high temperature resistant plastic bag (Figure 2.3 (b)) for autoclave consolidation (Figure 2.3 (c)).

In the autoclave, vacuum bagging (-450 to -650 mmHg) was applied with the consolidation temperature of 370°C, pressure of 8 bar, and a dwell time of 30 minutes to obtain uniform melting of the polymer layers. Then, these large plates of interlayer forms were cooled slowly (4°C/min) so that there would be sufficient time for the crystallization of the polymer layers.

When the autoclave consolidation was over, plates of interlayer forms were ready for demolding (Figure 2.3 (d)). Figure 2.3 (e) shows consolidated interlayer form plates while Figure 2.3 (f) indicates individual interlayer forms after cutting into strips. These strips of interlayer forms would be placed in between the lower and upper composite laminate strips during welding operations.

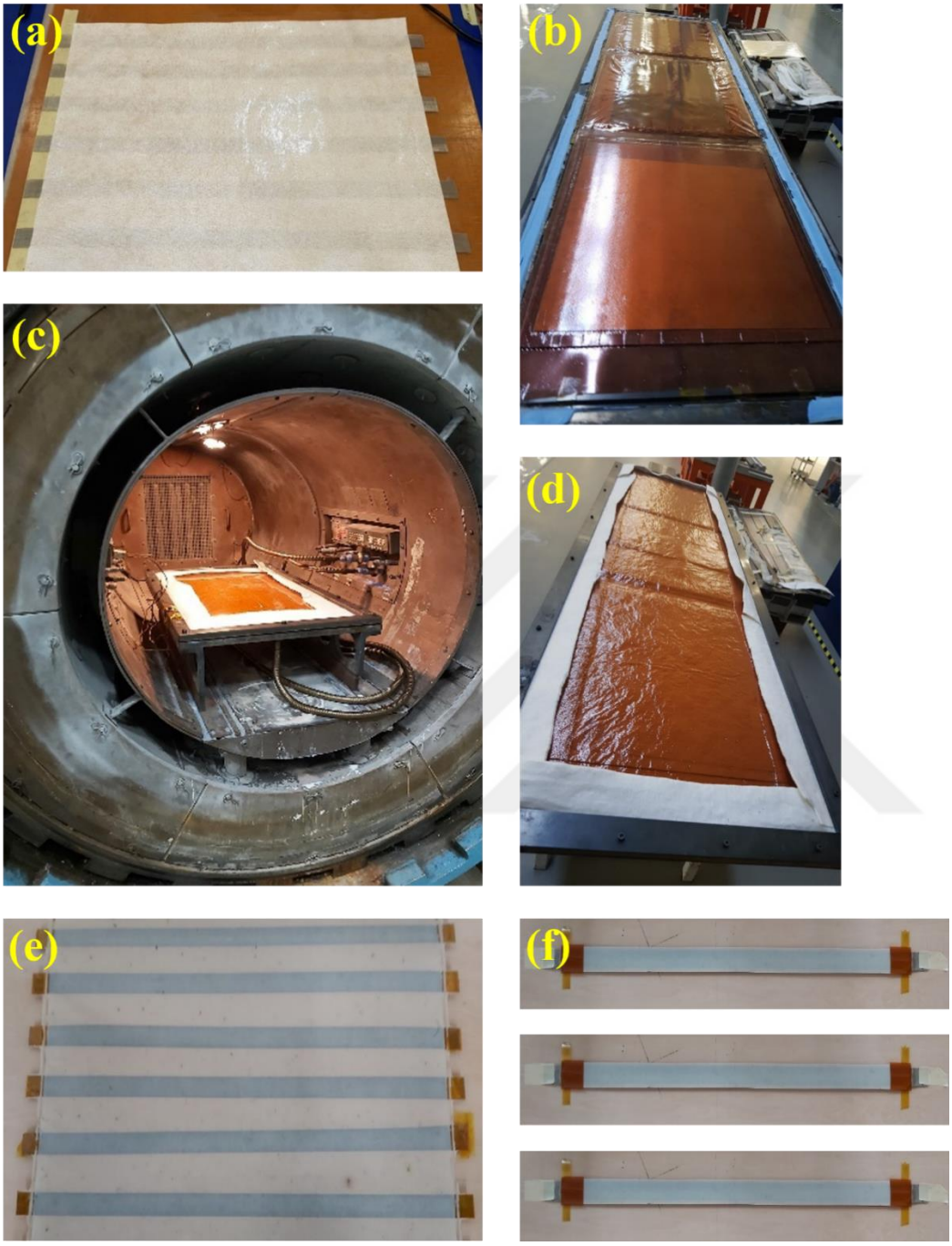

Figure 2.3 Steps during consolidation of the interlayer forms; (a) A plate of IF lay-up's on a tool, (b) Plastic bagging of the IF plate, (c) Consolidation in the autoclave, (d) IF plates after consolidation, (e) IF plate after demolding, and (f) IF strips after cutting.

2.4 Resistance Welding Operations

It is known that, as shown in Figure 2.4, during resistance welding operations of thermoplastic composite laminates under constant pressure, four thermal stages are required: Heating, Consolidation Melting, Crystallization, Cooling. Thus, for an efficient resistance welding operation, determination of the welding parameters; pressure level, power level, heating and cooling rate, dwell times of consolidation melting and matrix crystallization are crucial.

Therefore, for each six different interlayer forms, before starting resistance welding operations; several thermal studies were conducted to determine the optimum parameters of power level (voltage and amperage), heating and cooling rates, consolidation melting and crystallization dwell times, etc. The applied pressure was kept constant around 6 bars while the other consolidation parameter ranges required for melting and crystallization of the PAEK matrix were indicated in the time-temperature axes of Figure 2.4.

It should be noted that details of these preliminary thermal studies together with the optimum resistance welding parameters obtained for each configuration will be discussed in Chapter 3.

After determining the optimum parameters, resistance welding operations of the lower and upper PAEK/CF laminates with six different interlayer forms were conducted by using the welding system.

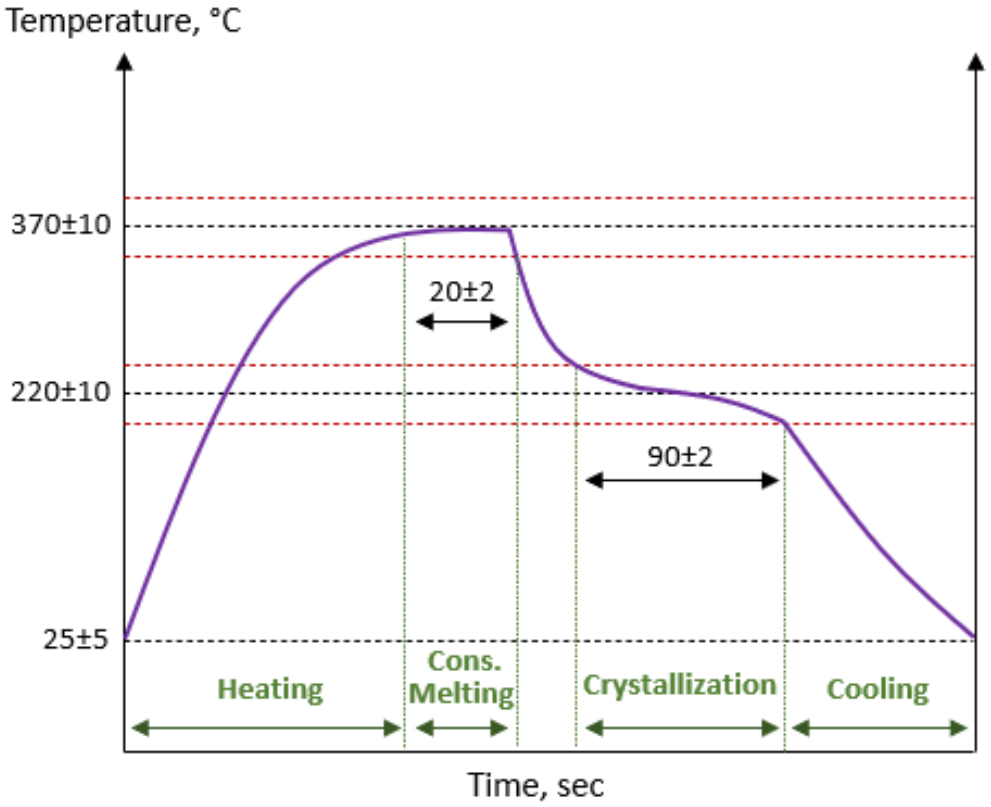

Figure 2.4 Typical Temperature - Time profile during four thermal stages required in resistance welding of the thermoplastic matrix composite laminates. Note that, values given in the axes are typical ranges for the PAEK matrix.

2.5 Ultrasonic Inspection and Machining of the Welded Specimens

After welding operations, all specimen groups were inspected for the possibilities of void formation and delamination. For this purpose, Automated Ultrasonic Through Transmission (AUTT) inspection technique was used via *Tecnotom Taurus Twin 2.0* system operated by properly qualified personnel. After examining the images of C-Scan maps obtained, certain suspicious regions were verified by using the Manual Ultrasonic Pulse Echo (MUPE) technique via *Olympus Omniscan SX* system.

Then, in accordance with the related standards, mechanical testing specimens were machined by using 5-axis CNC system (*CMS Advanced Materials Technology*) as shown in Figure 2.5.



Figure 2.5 Machining operation (above) and mechanical test specimen examples after machining (below).

2.6 Mechanical Testing of the Welded Specimens

In order to evaluate welding performance of the specimens having six different interlayer form configurations, mechanical tests were conducted to determine their "Interlaminar Fracture Toughness" and "Interlaminar Shear Strength" properties in accordance with the testing standards used for aerospace structures. Tests were conducted at laboratory conditions by using 250 kN capacity *Instron Universal Testing* system. For each specimen group four specimens were tested, and the properties were reported as average values with ± standard deviation.

(i) *Mode-I Interlaminar Fracture Toughness Energy (G_{IC}) Tests*

This test was conducted in accordance with the EN 6033 standard. The edge initial crack necessary was introduced by inserting a release film into the interface before the welding operations. Figure 2.6 shows the geometry of the specimen and Mode-I loading (opening mode) fixture, where total length (l) of the specimen was 250 mm while the initial crack length (a_i). i.e. length of the release film was 25 mm.

After obtaining the "Load versus Displacement" curve when a total of 100 mm propagated crack length (a) was reached, G_{IC} Fracture Toughness values were calculated by using the following relation:

$$G_{IC} = \frac{A}{a \times w} \times 10^6 \qquad (\mathrm{J/m^2})$$

Where;

A: Area (J) under the load (N) versus displacement (m) curve for total crack propagation.

a: Propagated crack length (100 mm)

w: Width of the specimen (25 mm)

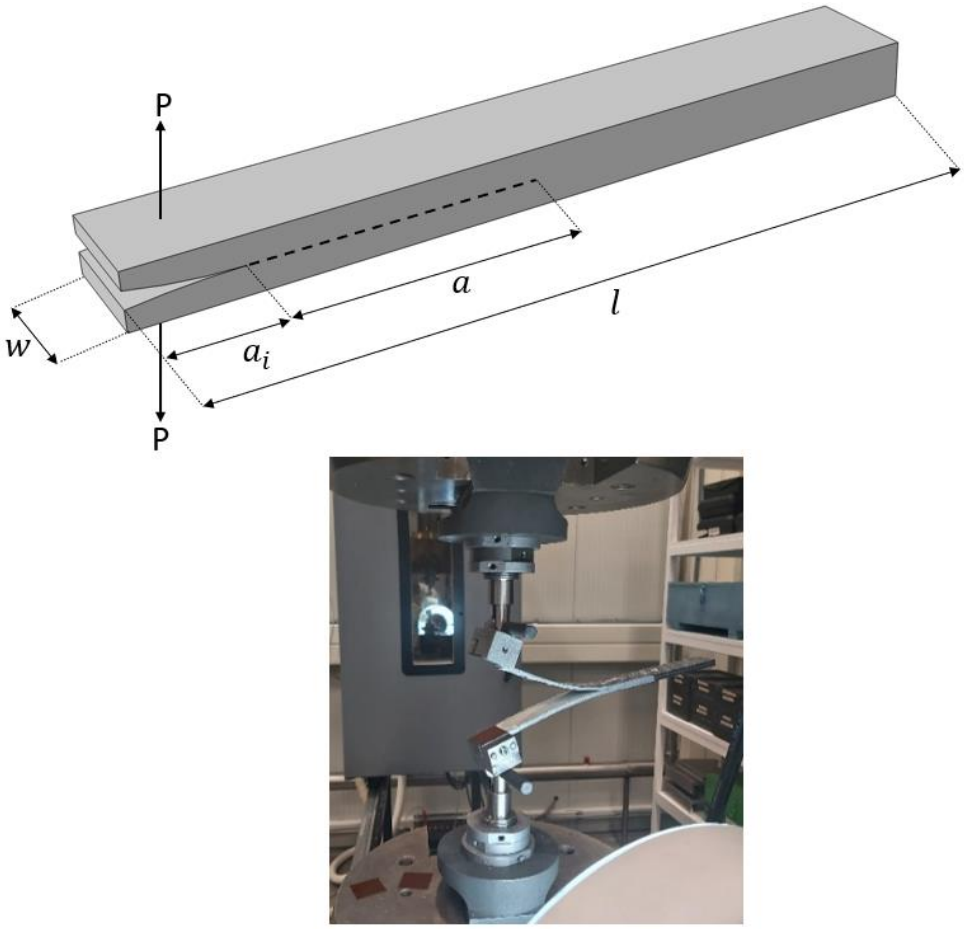

Figure 2.6 Specimen geometry (above) and Mode-I loading fixture (below) of the G_{IC} tests.

(ii) *Mode-II Interlaminar Fracture Toughness Energy (G_{IIC}) Tests*

This test was conducted in accordance with the EN 6034 standard. The edge initial crack necessary was introduced by inserting a release film into the interface before the welding operations. Figure 2.7 shows the geometry of the specimen having total length (l) of 165 mm together with the Mode-II loading (sliding mode) via three-point bending fixture.

During the test, "Load versus Displacement" curves were recorded until a sudden load drop was observed, which represents the start of "delamination" failure in the

weld interface. At this point, G_{IIC} Fracture Toughness values were calculated by using the following relation:

$$G_{IIC} = \frac{9 \times P \times a^2 \times d \times 1000}{2 \times w \times (\frac{1}{4L^3 + 3a^3})} \qquad (\mathrm{J/m^2})$$

Where;

d: Displacement value at the start of delamination (mm)

P: Load value for the start of delamination (N)

a: Initial crack length (40 mm)

w: Width of the specimen (25 mm)

L: Span length (100 mm)

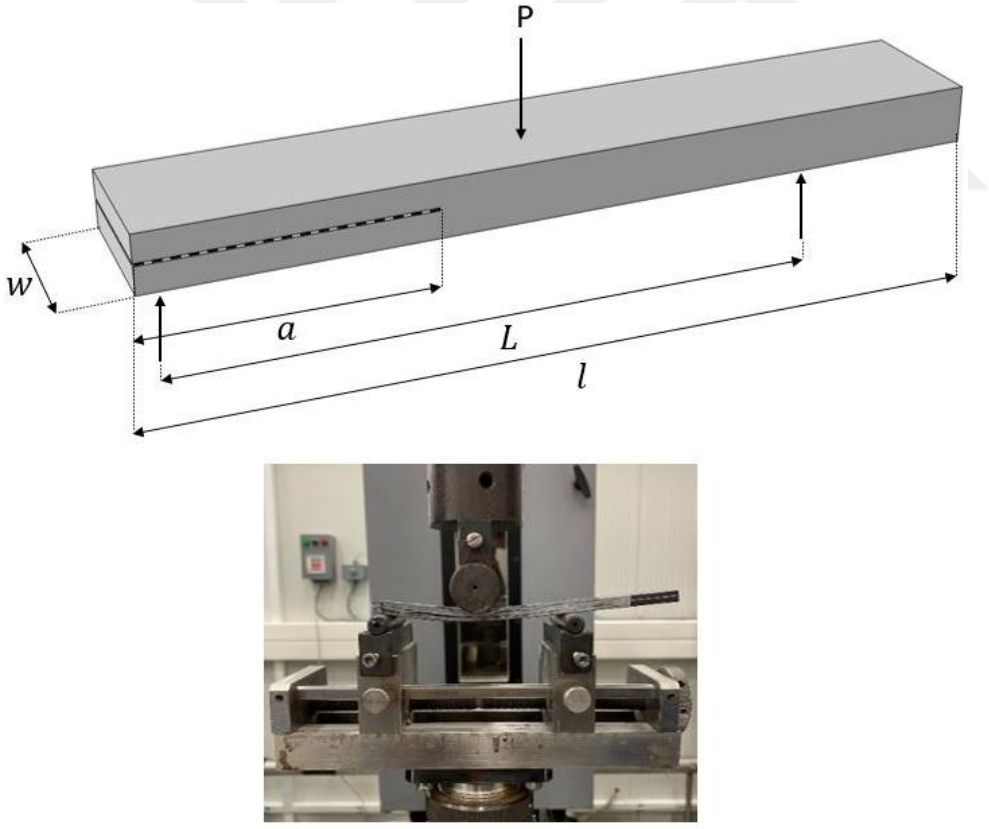

Figure 2.7 Specimen geometry (above) and Mode-II loading fixture (below) of the G_{IIC} tests.

(iii) ***Single Lap Shear Strength (SLSS) Tests***

This test was conducted in accordance with ASTM D5868 standard. Lap-shear regions, i.e. weld area of 25 x 12.5 mm, between the laminates were obtained by machining slots to the upper and lower welded laminates. Figure 2.8 indicates the geometry and the interfacial weld area under shear supplied by tensile load via fixtures initially separated (L) as 100 mm.

During the test, "Load versus Displacement" curves were recorded until the interlaminar shear failure occurred in the weld interface. Then, Single Lap Shear Strength (SLSS) values were calculated by using the following relation:

$$SLSS = \frac{P_{max}}{l \times w} \times 10^3 \qquad \text{(MPa)}$$

Where;

P_{max}: Maximum load applied (kN)

l: Length of the weld area (12.5 mm)

w: Width of the weld area (25 mm)

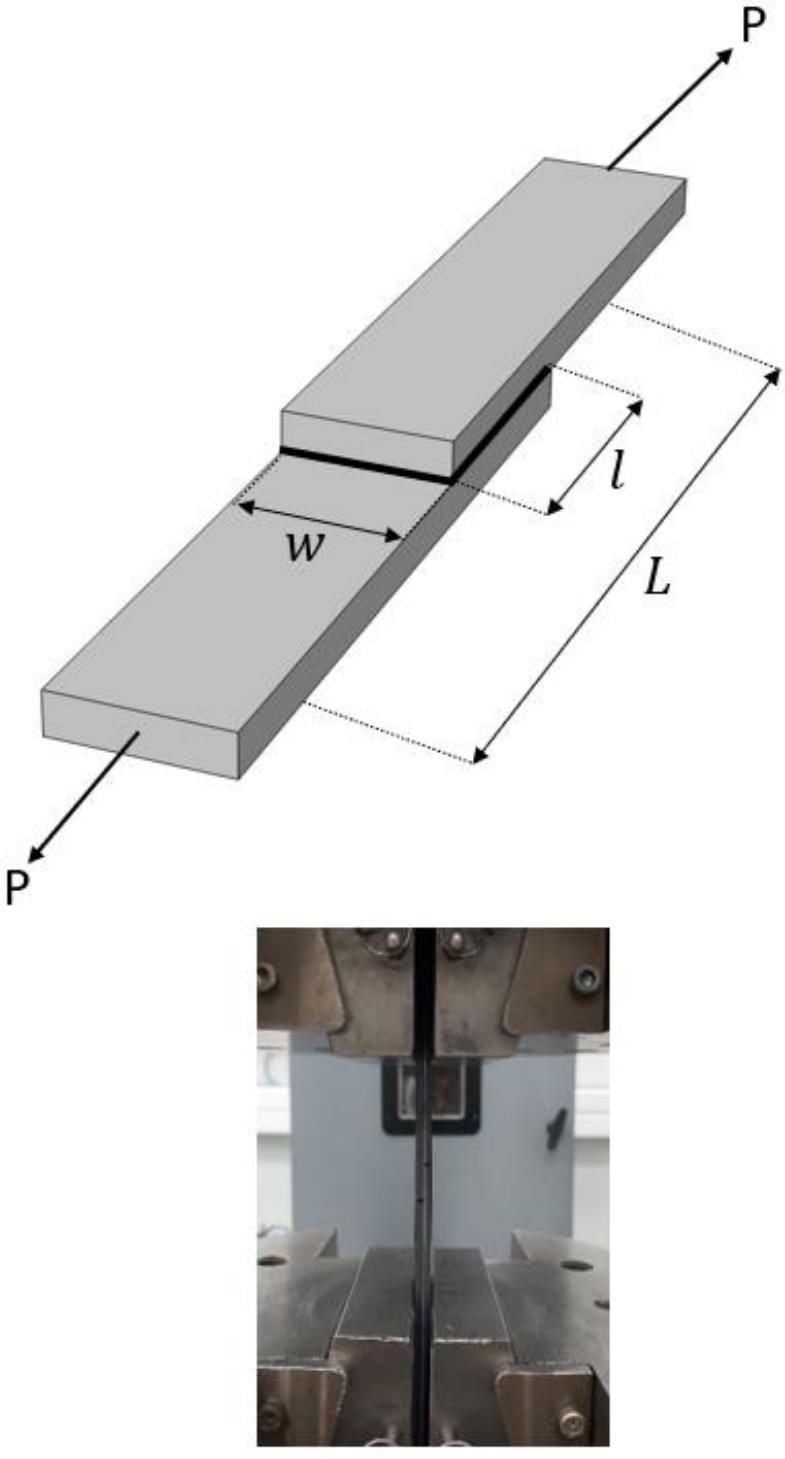

Figure 2.8 Specimen geometry (above) and tensile loading fixture (below) of the SLSS tests.

CHAPTER 3

RESULTS AND DISCUSSION

In this study, before welding operations, certain preliminary analyses were conducted to verify basic data on the upper and lower PAEK/CF laminates given by the supplier. Then, thermal profile studies were carried out to determine the welding parameters to be used for each interlayer form configurations. After welding, laminate strips were inspected by an ultrasonic non-destructive technique. In order to investigate effects of six different interlayer form configurations on the welding performance of the specimens, three different interlaminar tests were conducted. After mechanical tests, failure mode observations, microscopic examination and thermal analysis were also performed. Results of these experimental steps are discussed in the following sections.

3.1 Preliminary Analyses of the PAEK/CF Laminates

In this preliminary step, in order to verify basic data given by the supplier, three analyses were conducted for both lower and upper PAEK/CF laminates. Results of these analyses were all tabulated in Table 3.1 together with the suppliers data for comparison.

(i) *Fiber and Matrix Content Determination by Acid Digestion Method*

Contents of the fiber and matrix phases are very important key characteristics for composite materials; since the reinforcement (fiber) phase is the main load carrier allowing the composite material to endure against mechanical loads and stresses while the matrix is the other crucial phase to transfer the applied loads to the strong reinforcements.

In this study, fiber and matrix content of the PAEK/CF laminates to be welded were determined by conducting acid digestion method. At least three measurements were carried out for both upper and lower laminates in accordance with the procedure given in the experimental part. Average values of the fiber and matrix contents together with densities are tabulated in Table 3.1.

It was seen that density of the lower and upper laminates were 1.58 and 1.53 g/cm^3 while their fiber contents were 58.5 and 51.5 vol%, and their matrix contents were 34.5 and 40.6 wt%, respectively. All the values determined were consistent with the suppliers data.

(ii) ***Thickness and Porosity Determination by Optical Microscopy***

Before starting welding operations, it was also important to verify given thicknesses of the upper and lower PAEK/CF laminates including the possible microstructural defects such as porosity. Therefore, upper and lower laminates used in this study were first inspected by using an optical microscope with an image analyses software to observe porosity and to measure the thicknesses of the laminates precisely.

At least three examinations and measurements were conducted for the upper and lower laminates, and the calculations were done as explained in the experimental part. Figure 3.1 shows an example of the through-thickness optical microscope image analyses for precise thickness measurements and porosity determination for the upper and lower laminates. Note that thickness measurements were done at least from three different locations of the cross-sectional views of the laminate thicknesses.

Table 3.1 indicated that the precise thickness of the lower laminate was 3.06 mm with a thickness deviation of -1.12 % while these values for the upper laminate were 2.38 mm and -0.06 %, respectively. Porosity level determined with the image

analysis software for each plate were only 0.02 %. These measurements were again consistent with the suppliers data.

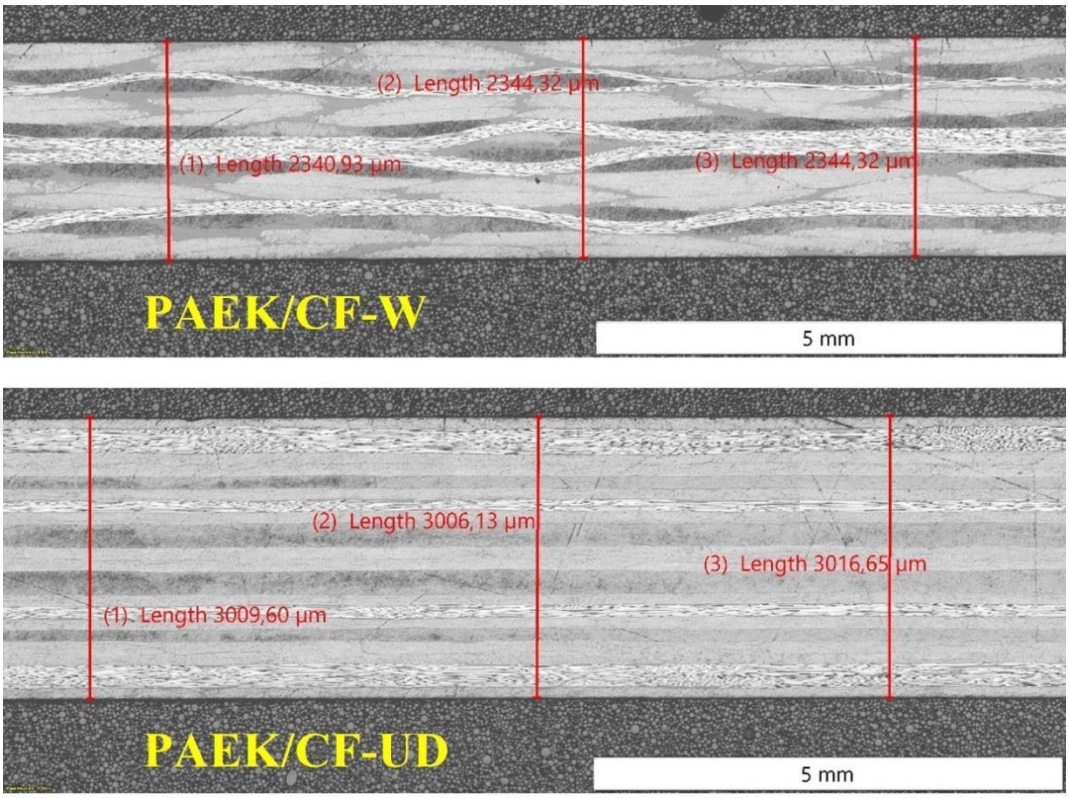

Figure 3.1 Example of the through-thickness optical microscope image analysis for the upper and lower PAEK/CF laminates.

(iii)*Glass Transition and Crystallinity Determination by DSC Analyses*

In order to assess Glass Transition Temperature (T_g) Range and Crystallinity (X_c) degree of the PAEK matrix in the composite laminates to be welded, DSC analyses were conducted according to the procedure presented in the experimental part. At least three analyses were conducted for the upper and lower laminates. One example of the first heating DSC thermograms for each laminate are shown in Figure 3.2 while the glass transition temperature range and crystallinity degree of their PAEK matrix are tabulated also in Table 3.1.

It is seen in Table 3.1 that T_g range of the laminates were between 134-160°C while their matrix crystallinity X_c were around 26 %. These values were again consistent with the suppliers data.

Moreover, it should be pointed out that, as shown in Figure 3.2, during the first heating no cold crystallization enthalpy (ΔH_{cc}) was observed. This could be interpreted as the use of proper consolidation parameters (i.e. proper temperature levels and dwell times) during the production of the PAEK/CF laminates by the supplier.

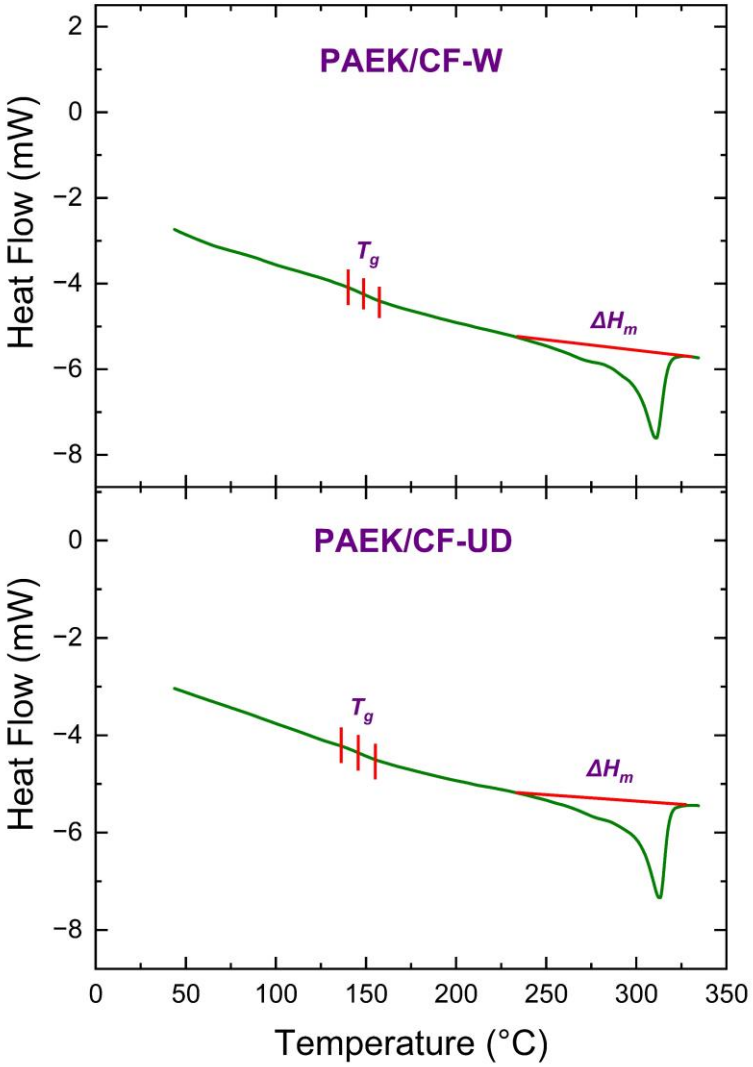

Figure 3.2 Example of the first heating DSC thermograms for the upper and lower PAEK/CF laminates.

Table 3.1 Results of the three preliminary analyses conducted for the upper and lower PAEK/CF laminates before welding. Note that the last column in the table gives the suppliers data for comparison.

Analyses	**Properties**	**Unit**	**PAEK/CF-UD**	**PAEK/CF-W**	**Suppliers Data**
Acid Digestion	Density	g/cm^3	1.58	1.53	1.55 ± 0.05
	Fiber Content	vol%	58.40 ± 0.99	51.50 ± 0.65	58±3 & 52±3
	Matrix Content	wt%	34.47 ± 1.12	40.66 ± 0.78	34±3 & 42±3
Optical Microscopy	Thickness	mm	3.06 ± 0.03	2.38 ± 0.03	3.10 & 2.40
	Thickness Deviation	%	-1.12	-0.06	±5
	Porosity	%	0.02	0.02	±2
DSC	T_g range	°C	137 - 158	134 - 160	125 - 175
	Crystallinity	%	25.66 ± 1.58	26.63 ± 0.58	17 - 30

3.2 Determination of the Resistance Welding Parameters for Each Interlayer Forms

As explained in the experimental part (Section 2.4), for an efficient resistance welding operation proper temperature-time profile should be used during the four stages of consolidation: Heating, melting, crystallization, cooling. As shown in Figure 2.4, for the homogenous melting (370 ±10°C) and proper hot crystallization (220 ±10°C) temperatures, dwell times for melting and crystallization of the PAEK matrix were determined as 20 sec and 90 sec, respectively; under the power level of 50 V and pressure level of 6 bars.

Then, in order to determine optimum "amperage" levels required for the heating, melting and crystallization stages of the six different Interlayer Forms, several temperature-time profile studies were conducted by placing thermocouples into the three different locations between the upper PAEK/CF laminates and Interlayer Forms.

One example of these temperature-time profiles obtained from three different thermocouples for the IF-1 Interlayer Form is given in Figure 3.3. Note that, these curves were all in accordance with the typical temperature-time profiles of the resistance welding of PAEK/CF laminates given in Figure 2.4 in the experimental procedures section.

After obtaining all the temperature-time profiles for each Interlayer Forms, optimum "amperage" parameters required for the welding consolidation stages of heating, melting and crystallization were determined and tabulated in Table 3.2 together with the Heating Duration times.

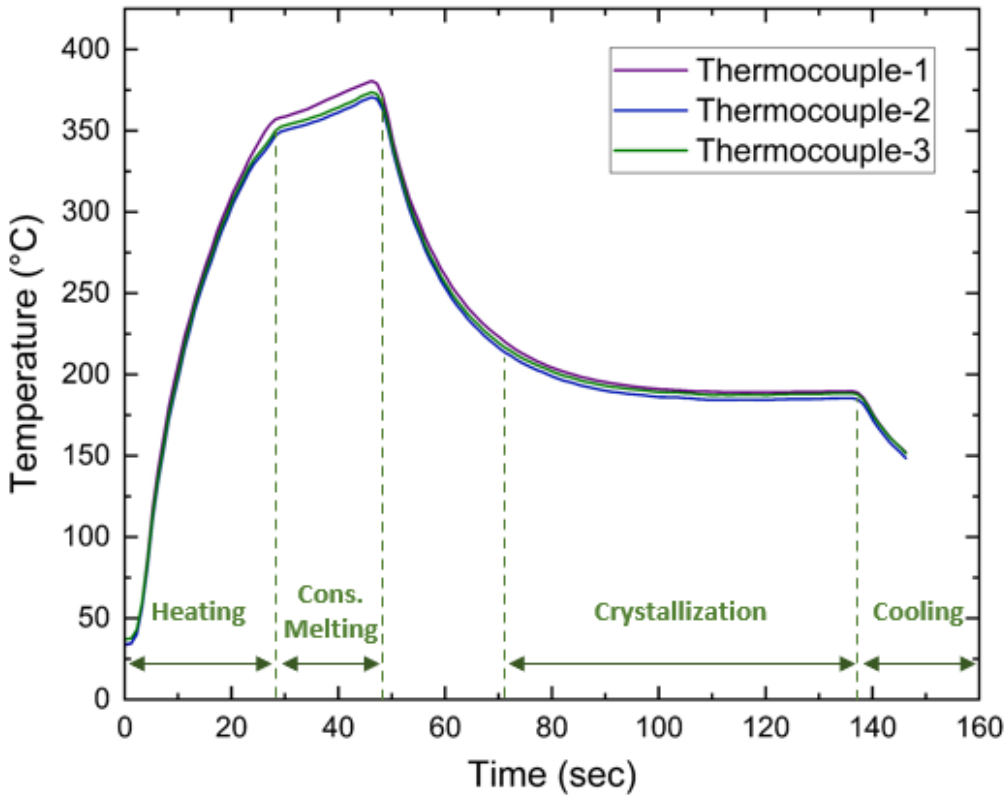

Figure 3.3 Example of the temperature-time profile obtained from three different thermocouples for the IF-1 Interlayer Form.

Table 3.2 Optimum amperage parameters determined for the resistance welding operations of Six different Interlayer Forms.

Interlayer Forms	Heating Amperage (A)	Heating Duration (sec)	Cons. Melting Dwell Amperage (A)	Crystallization Dwell Amperage (A)
IF-1 (HE1-IG1)	100	25	90	50
IF-2 (HE1-IG2)	96	28	89	52
IF-3 (HE1-IG3)	93	30	87	52
IF-4 (HE2-IG1)	55	40	45	28
IF-5 (HE2-IG2)	50	40	43	26
IF-6 (HE2-IG3)	46	40	40	25

3.3 Ultrasonic Inspection of the Welded Specimens

After welding operations, before the mechanical tests, in order to reveal possibilities of void formation and delamination, welded laminate strips were inspected by Automated Ultrasonic Through Transmission (AUTT) and Manual Ultrasonic Pulse Echo (MUPE) techniques. For six different Interlayer Forms, four welded laminate strips were inspected according to the procedure given in the experimental work section.

Then, images obtained in the form of C-Scan mapping (Figure 3.4 and Figure 3.5) from the AUTT inspection were evaluated. Figure 3.4 and Figure 3.5 generally show that IF-1 and IF-4 Interlayer Forms with IG1 Insulating Glass Fiber layer (having the highest areal weight) had rather uniform color mapping while the other Interlayer Forms with IG2 and IG3 insulating layers (having lower areal weights) had C-Scan maps with certain degree of suspicious areas having sound wave attenuations (decibel losses). After the C-Scan mapping, MUPE technique was also used to confirm the sound wave attenuations detected during AUTT inspection.

Therefore, as will be discussed in the following section, those welded specimens with IF-1 and IF-4 interlayer forms (having IG1 insulating layer) resulted in higher mechanical performance. On the other hand, other Interlayer Form configurations having IG2 and IG3 insulating layers resulted in lower interlaminar properties.

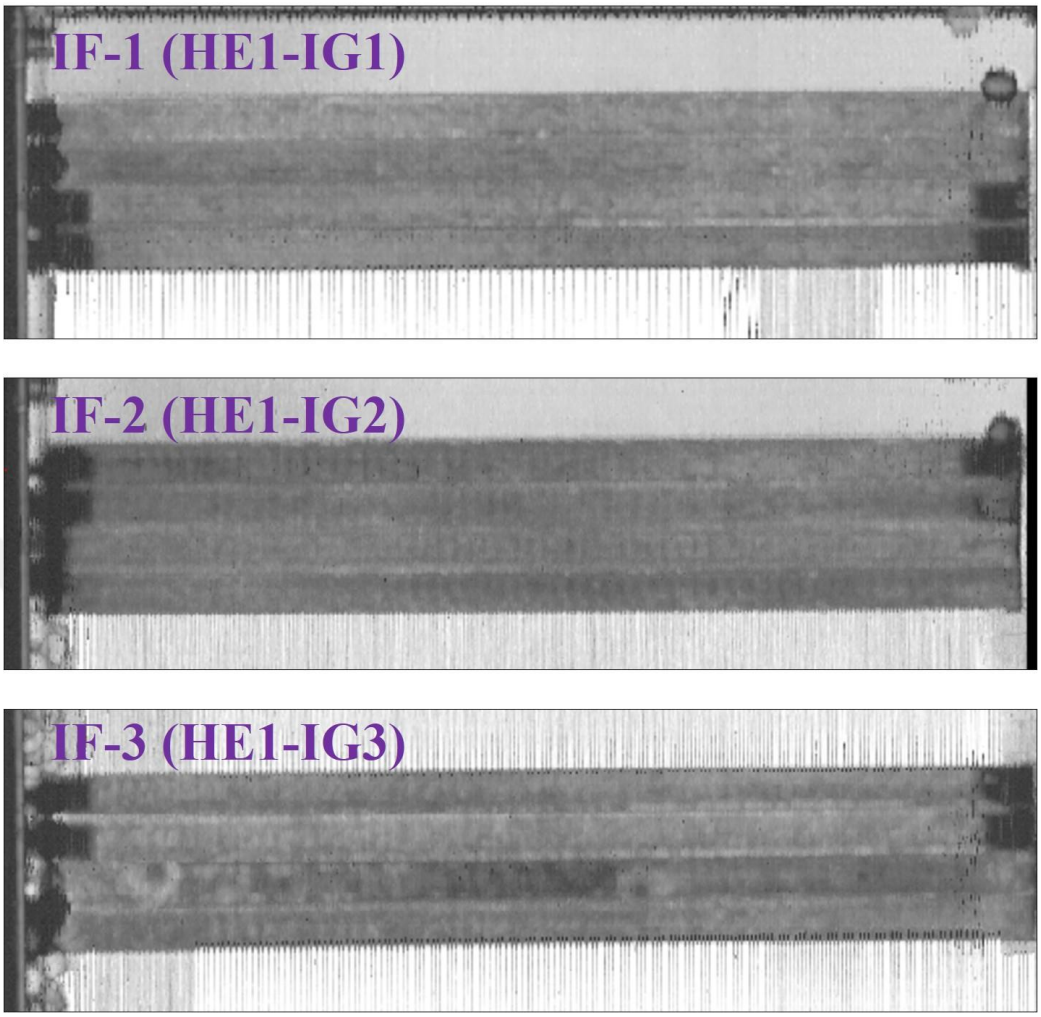

Figure 3.4 C-scan images obtained from the AUTT inspection of the four welded strips for each IF-1, IF-2 and IF-3 Interlayer Forms.

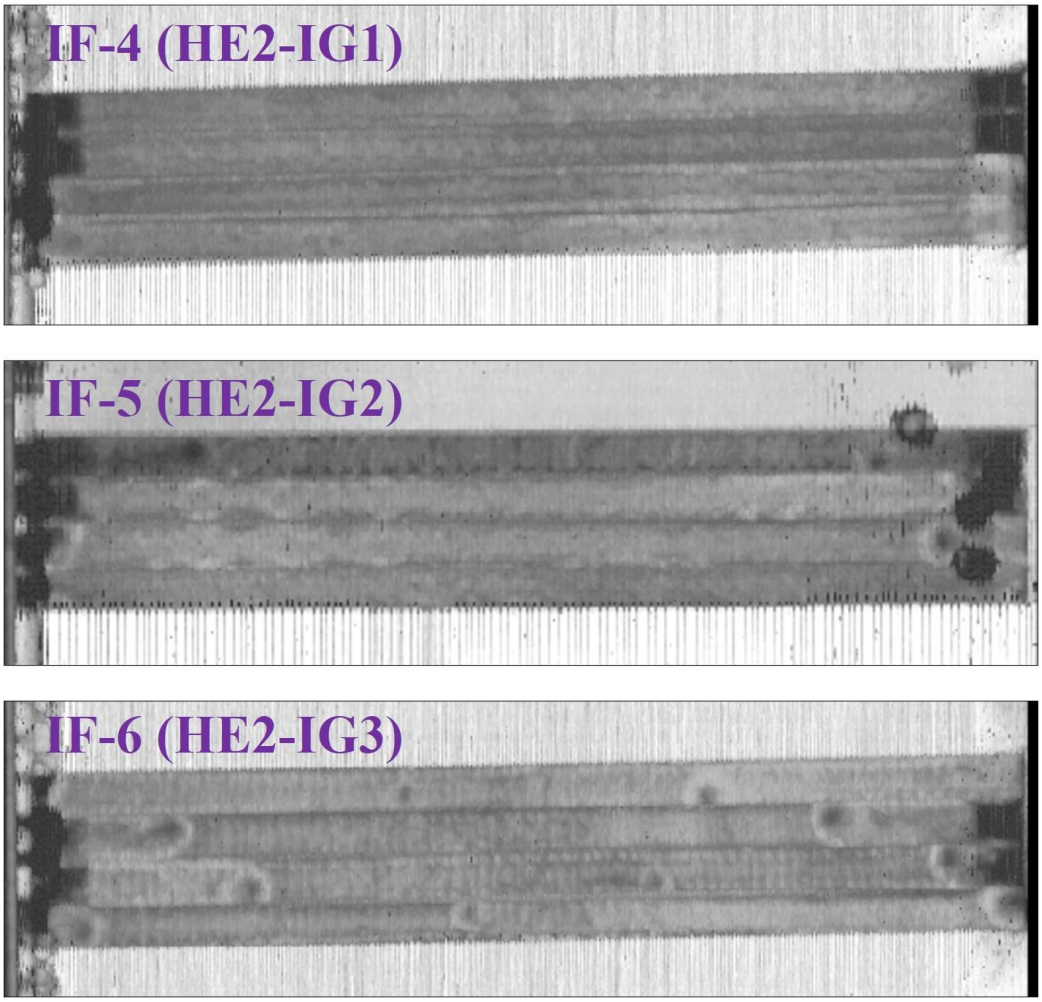

Figure 3.5 C-scan images obtained from the AUTT inspection of the four welded strips for each IF-4, IF-5 and IF-6 Interlayer Forms.

3.4 Effects of Interlayer Forms on the Mechanical Performance of Welded Specimens

In this study, effects of interlayer forms on the mechanical performance of welded specimens were investigated by conducting three tests; Interlaminar Fracture Toughness Energy under Mode-I (G_{IC}) and Mode-II (G_{IIC}), and Single Lap Shear Strength (SLSS). After obtaining load versus displacement curves during these tests (Figure 3.6), mechanical properties of G_{IC}, G_{IIC} and SLSS were calculated for the specimens having six different Interlayer Forms. Average values with standard deviations are evaluated in Figure 3.7 and Table 3.3.

It is clearly seen that welded specimens with IF-1 interlayer form had the highest level of mechanical performance. Their G_{IC}-G_{IIC} Interlaminar Fracture Toughness values were as much as 3.76 and 4.71 kJ/m^2, respectively. Similarly, their SLSS Interlaminar Shear Strength was as much as 37 MPa. It is known that these mechanical performances could be sufficient for many structural applications made from composite laminates.

Figure 3.7 and Table 3.3 also indicated that welded specimens with IF-4 interlayer form had similarly high-level mechanical performance with the ones having IF-1 interlayer form. The only difference between these Interlayer Forms is their "Heating Element" layers designated as HE1 and HE2.

As tabulated in Table 2.4, both HE1 and HE2 layers are made of "Stainless Steel Meshes", having certain differences in terms of "Mesh Style" and "Areal Weight". Since both of them resulted in higher level of mechanical performance, it could be stated that use of these two different Stainless Steel Mesh forms as Heating Element layers (HE1 and HE2), could be considered as an appropriate choice in the resistance welding of PAEK/CF thermoplastic composite laminates.

The common layer in IF-1 and IF-4 interlayer forms was their "Insulating Layer" designated as IG1, which is actually a "Woven Glass Fiber" layer impregnated with

the matrix resin. Thus, it could be interpreted that the main reason of having very high-level mechanical performance in the welded specimens with IF-1 and IF-4 interlayer forms should be due to their common IG1 insulating layer.

On the other hand, Figure 3.7 and Table 3.3 revealed that those welded specimens having IG2 and IG3 insulating layers in their Interlayer Forms had rather lower-level mechanical performance. For instance, welded specimens with IF-6 interlayer form (i.e. having IG3 insulating layer) had the lowest mechanical properties. Their G_{IC} and G_{IIC} Interlaminar Fracture Toughness values were as low as 1.82 and 2.62 kJ/m^2, respectively. Similarly, their SLSS Interlaminar Shear Strength was as low as 16 MPa. These decreases, compared to the welded specimens with IF-1 were -51 %, -44 % and -56 %, respectively.

Then, it could be pointed out that, in the resistance welding of PAEK/CF laminates, if Stainless Steel Mesh layers were used as the Heating Element, then the type of the Woven Glass Fiber layer as the Insulating Layer become very crucial. For instance, use of IG1 could be considered a perfect choice compared to the lower performance of IG2 and IG3.

What is the difference between the IG2, IG3 and IG1? Table 2.5 indicates that although all of them are made of woven E-glass fibers, the differences are their "Fiber Diameter", being 6 μm for IG1 and 5 μm for the others; and more significantly their "Areal Weight", being 296 gsm for IG1 and only 105 gsm and 48 gsm for the others. This means that during resistance welding operations, use of thicker and heavier Woven Glass Fiber insulating layers would perform their functions much more properly and efficiently.

It is known that during resistance welding the main function of the electrically "Insulating Layer" present in the "Interlayer Form" was to prevent current leakage to the other layers in the composite laminate. This phenomenon is called "Current Leakage" problem being one of the significant issue during resistance welding operations. Because if current leakage occurs to the upper or lower composite

laminates during welding, then not only voids could form in the thermoplastic matrix, but also delamination might occur in the upper or lower composite laminates being welded.

Apart from “Current Leakage” problem, another issue encountered during resistance welding operations is named as “Short-Cut” problem. This problem takes place if the Stainless-Steel Mesh heating element touches to the carbon fiber reinforcement present in the upper or lower composite laminates. Since carbon fiber reinforcements have certain degree of electrical conductivity, current in the Stainless-Steel Mesh heating element would pass to the carbon fiber reinforcements, leading to “Short-Cut” in the welding interface. Due to the loss in the magnitude of the current, melting stage of the welding would not take place properly, resulting in improper welding.

Of course, these two problems (Current Leakage and Short-Cut) directly depend on the efficiency of the Insulating Layers. If Insulating Layers (IGs) electrically insulate the Heating Element layers (HEs) properly from the upper and lower composite laminates, then these issues would be not significant.

Therefore, it can be concluded that, in this study, use of rather thicker and heavier Woven Glass Fiber insulating layers, i.e. use of IG1, was very efficient to prevent problems of Current Leakage and Short-Cut during resistance welding operations of PAEK/CF composite laminates.

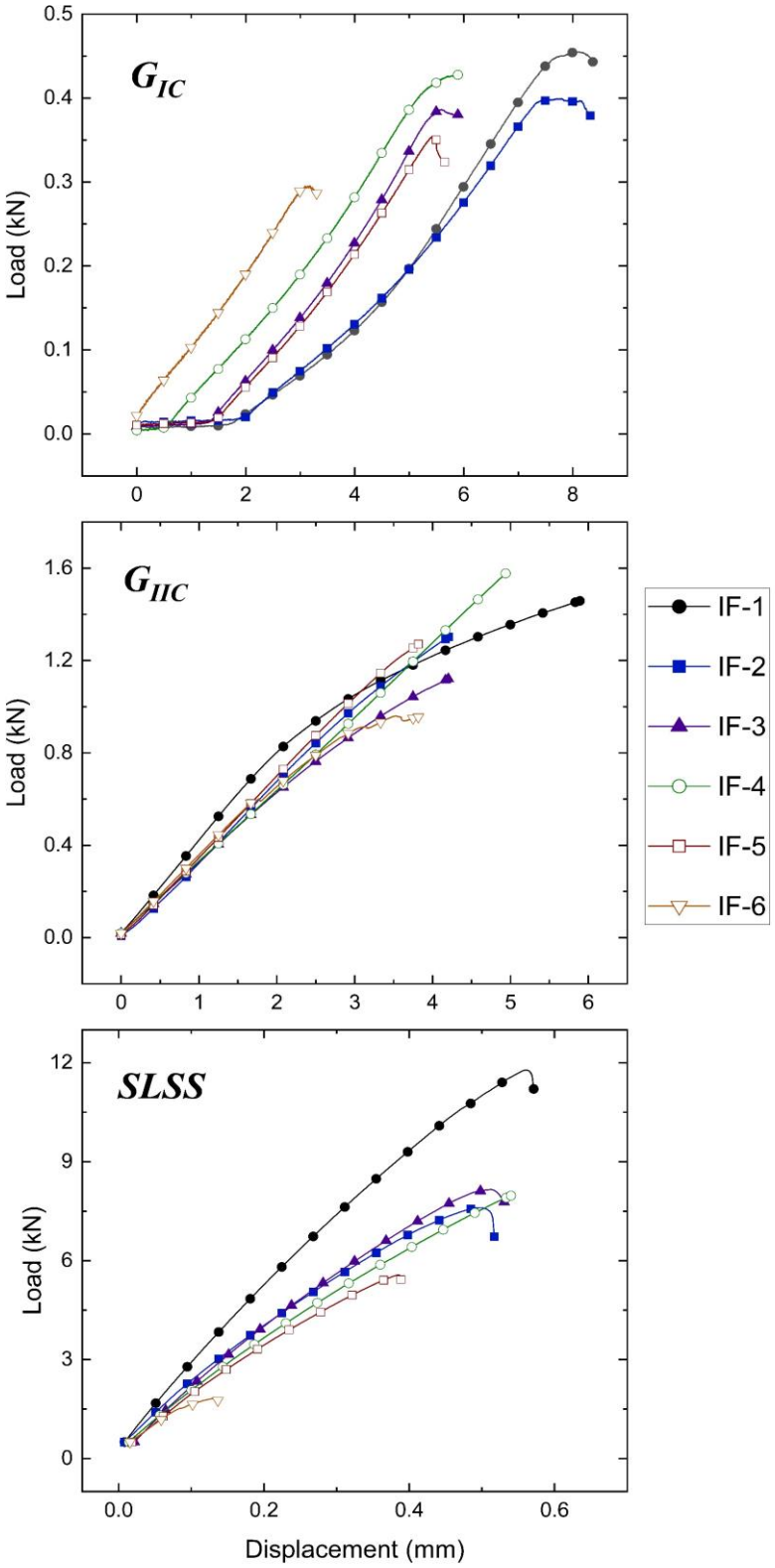

Figure 3.6 Load vs. displacement curves obtained during G_{IC}, G_{IIC} and SLSS tests.

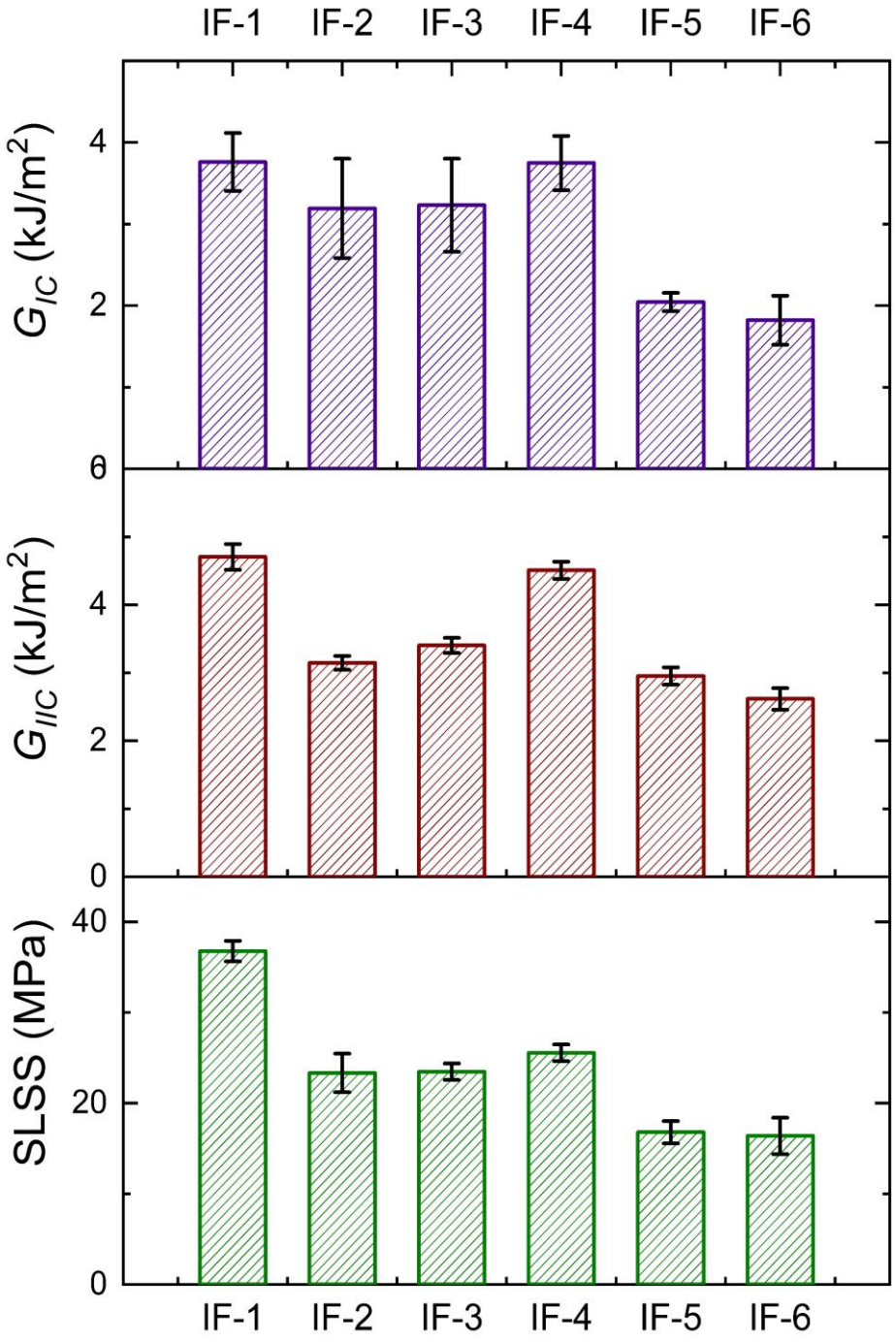

Figure 3.7 Effects of Interlayer Forms on the interlaminar fracture toughness (G_{IC}, G_{IIC}) and shear strength (SLSS) values of the welded specimens.

Table 3.3 Average values of the interlaminar fracture toughness (G_{IC}, G_{IIC}) and interlaminar shear strength (SLSS) values of the welded specimens with six different Interlayer Forms.

Interlayer Forms	G_{IC} (kJ/m^2)	G_{IIC} (kJ/m^2)	SLSS (MPa)
IF-1 (HE1-IG1)	3.76 ± 0.36	4.71 ± 0.19	36.77 ± 1.14
IF-2 (HE1-IG2)	3.19 ± 0.61	3.15 ± 0.10	23.33 ± 2.14
IF-3 (HE1-IG3)	3.23 ± 0.57	3.40 ± 0.11	23.47 ± 0.91
IF-4 (HE2-IG1)	3.75 ± 0.33	4.51 ± 0.13	25.55 ± 0.92
IF-5 (HE2-IG2)	2.04 ± 0.11	2.95 ± 0.13	16.80 ± 1.23
IF-6 (HE2-IG3)	1.82 ± 0.30	2.62 ± 0.16	16.40 ± 2.01

3.5 Interlaminar Failure Modes Observed During Testing of Welded Specimens

It is known that when welded composite laminates are loaded; depending on the weld quality and the applied load direction, "interlaminar failure" might occur in various ways. As shown in Figure 3.8, after interlaminar fracture toughness tests (such as G_{IC}, G_{IIC}) and interlaminar shear strength tests (such as SLSS), generally four typical interlaminar failure modes are observed; (i) cohesive failure, (ii) adhesive failure, (iii) delamination failure and (iv) mixed failure (i.e. mixture of the others). In this study, after all mechanical tests, interlaminar failure modes of the welded specimens were examined. Typical examples observed during G_{IC}, G_{IIC} and SLSS tests are given in Figure 3.9, Figure 3.10 and Figure 3.11, respectively.

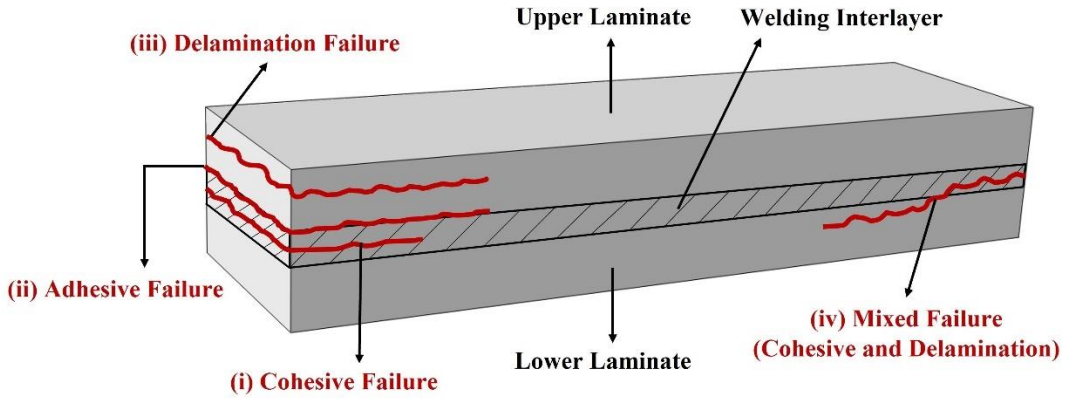

Figure 3.8 Four typical interlaminar failure modes; (i) cohesive, (ii) adhesive, (iii) delamination and (iv) mixed failure that might be observed during the mechanical tests of welded specimens.

"Cohesive Failure" is defined as the failure i.e. crack propagation along the welding interlayer which represents high quality of the welding operation because the interlaminar failure is not taking place between the weld and the upper or lower composite laminate. In this study, Cohesive Failure was especially observed in the specimens having IF-1 and IF-4 interlayer forms. In this mode, as shown in Figure 3.9 and Figure 3.11, weld adherent was observed on both sides (upper and lower) of the joined laminates. It should be noted that these specimens (having IF-1 and

IF-4 interlayer forms) also had the highest mechanical properties as discussed before.

“Adhesive Failure” is defined as the failure i.e. crack propagation in between the welding interlayer and upper or lower composite laminates, which represents lower quality of the welding operation because this means that intertwining mechanism between the macromolecular chains present in the PAEK matrix of welding interlayer and the PAEK matrix of the upper or lower composite laminate is not occurring properly. As shown in Figure 3.9, Figure 3.10 and Figure 3.11, in some of the welded specimens (such as IF-2 and IF-3) having rather lower mechanical properties, Adhesive Failure mode was observed.

“Delamination Failure” is defined as the failure i.e. crack propagation totally through the interlayers of the upper or lower composite laminates, not related to the welding interlayer. This type of interlaminar separation in the welded composite specimens could be due to the problems encountered during specimen production, specimen cutting, improper testing loads, etc. In this study, that kind of interlaminar failure was observed in very limited number of specimens, one example is shown in Figure 3.10 for the IF-5 specimen. Since this failure mode is not related to the welding operation, their mechanical properties obtained were not included in the average values.

It is known that apart from cohesive, adhesive and delamination failure modes, there is another possibility in the welded composite laminates, which is named as “Mixed Failure”, i.e. a mixture of the other three. In this study, that type of mode was observed in the form of “Cohesive/Delamination Failure” mixture, especially in some of the specimens having IF-5 and IF-6 interlayer forms, as indicated in Figure 3.9 and Figure 3.11. In this mode, cracks propagate both in the welding interlayer and in the upper or lower composite laminates. The main reason for this behavior was, as also observed in the C-Scan images of these specimens, presence of the interior defects in the upper and lower composite laminates. Since their

Insulating Layers were IG2 or IG3, it was difficult to prevent the "Current Leakage" problem discussed before.

Therefore, welded specimens having IF-5 and IF-6 interlayer forms had the lowest mechanical properties.

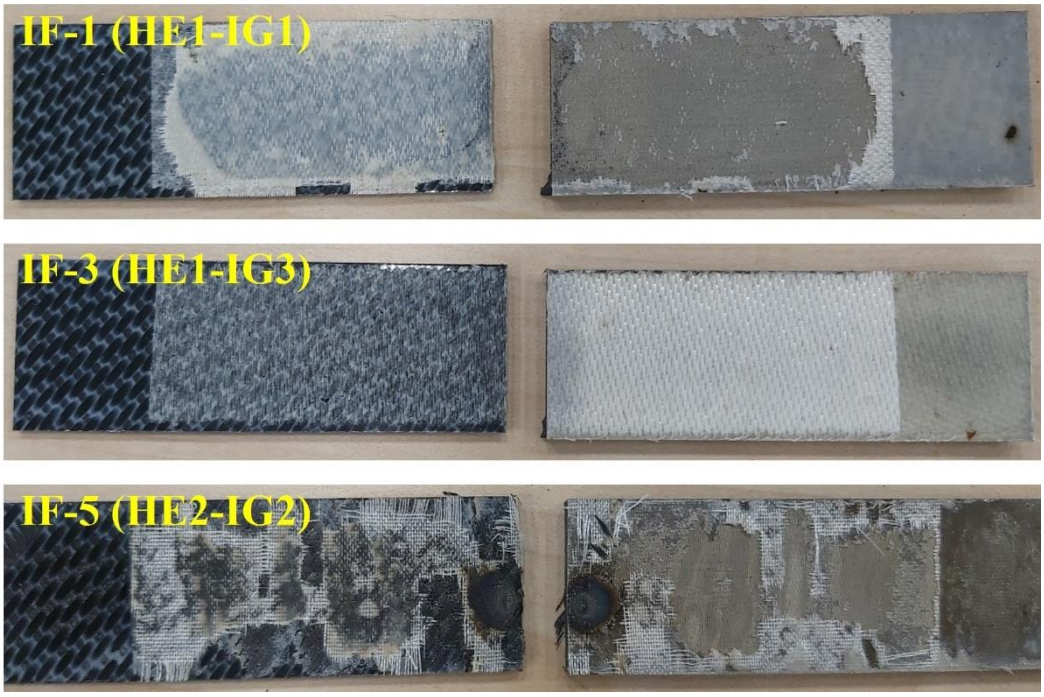

Figure 3.9 Examples of interlaminar failure modes observed during G_{IC} tests. From top to down: Cohesive, adhesive, mixed (cohesive and delamination).

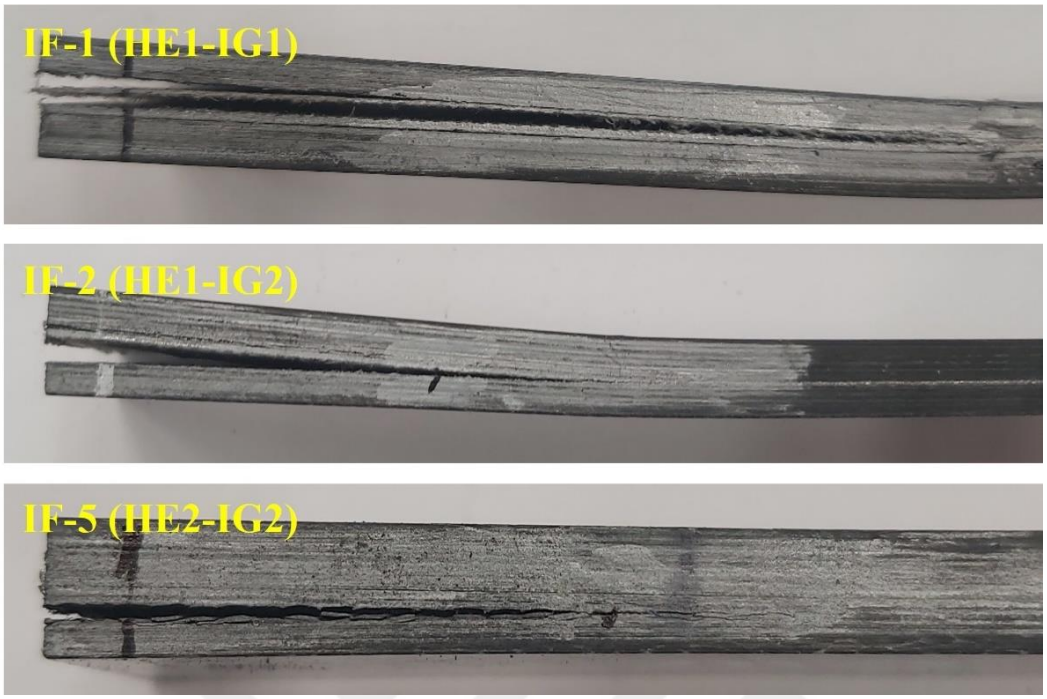

Figure 3.10 Examples of interlaminar failure modes observed during G_{IIC} tests. From top to down: Cohesive, adhesive, delamination.



Figure 3.11 Examples of interlaminar failure modes observed during SLSS tests. From top to down: Cohesive, adhesive, mixed (cohesive and delamination).

3.6 Microscopic Analyses of the Welded Specimens

In order to assess whether there were any significant changes or not in the Thickness Deviation and Porosity Level of the specimens “after” welding operation, optical microscope inspection with an image analysis software was conducted for all specimens having six different Interlayer Forms. At least three examinations and measurements were taken for each specimen.

As shown in Figure 3.12, total thickness of the specimens before and after welding was determined as the summation of the thicknesses of Upper Laminate + Interlayer Form + Lower Laminate. Then, average values of the “Thickness Deviation” and the “Porosity Level” in percentages were tabulated in Table 3.4.

It was observed that Thickness Deviation of the specimens after welding was in the range between 1.1 % and 1.7 %, which could be considered as an acceptance range.

Table 3.4 also revealed that, compared to others, specimens with IF-1 and IF-4 interlayer forms after welding had rather lower Porosity Levels being only 1.17 % and 1.25 %. Thus, as discussed before, those welded specimens having IF-1 and IF-4 performed with the highest mechanical properties.

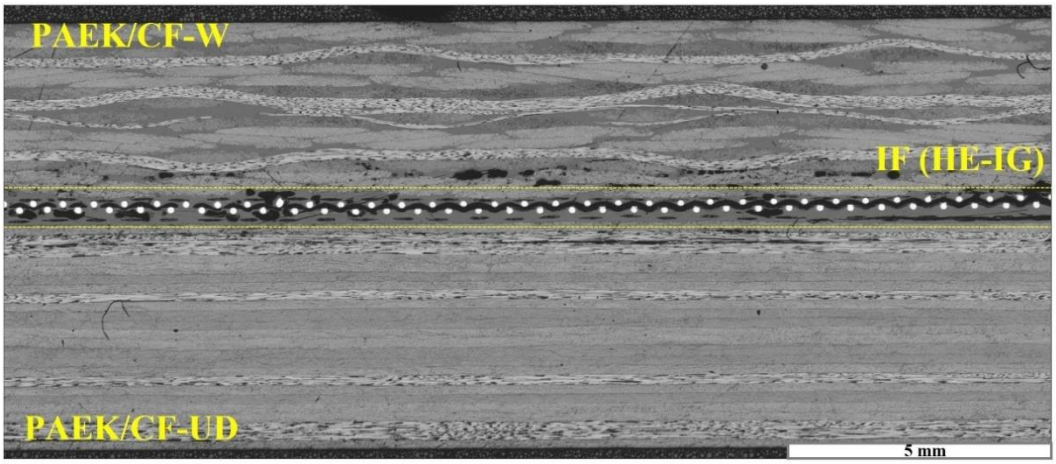

Figure 3.12 One example of the through-thickness optical microscope image analysis conducted after welding.

Table 3.4 Average Thickness Deviation and Porosity Level after welding of the specimens with six different interlayer forms.

Interlayer Forms	Thickness After Welding (mm)	Thickness Deviation (%)	Porosity (%)
IF-1 (HE1-IG1)	6.18 ± 0.02	1.14 ± 0.27	1.17 ± 0.13
IF-2 (HE1-IG2)	5.90 ± 0.09	1.26 ± 1.49	1.67 ± 0.21
IF-3 (HE1-IG3)	5.87 ± 0.13	1.71 ± 2.26	1.43 ± 0.57
IF-4 (HE2-IG1)	6.01 ± 0.01	1.11 ± 0.19	1.25 ± 0.24
IF-5 (HE2-IG2)	5.79 ± 0.08	1.28 ± 1.70	1.90 ± 0.41
IF-6 (HE2-IG3)	5.74 ± 0.04	1.36 ± 0.76	1.39 ± 0.24

3.7 DSC Analyses of the Welded Specimens

In order to reveal whether there were any significant changes or not in the Glass Transition Temperature (T_g) range and Crystallinity Degree (X_c) of the PAEK matrix after welding operations, DSC analyses were conducted for all welded specimens with six different interlayer forms. For each group, at least three analyses were performed by taking the samples carefully from around the welding interface. Examples of the first heating thermograms are given in Figure 3.13 while the T_g range and average values of X_c for each specimen are tabulated in Table 3.5.

Figure 3.13 revealed that, just like the DSC analyses conducted for the upper and lower PAEK/CF laminates before welding, as discussed in Section 3.1, Figure 3.2, during the first heating no cold crystallization enthalpy (ΔH_{cc}) was observed after the welding operations.

Table 3.5 indicated that T_g range of the specimens after welding is 137-163°C while their average crystallinity degree is between 24-27 %. It was seen that these T_g and X_c values were very close to the values obtained before welding, as discussed before in Section 3.1 Table 3.1.

Table 3.5 Glass Transition Temperature (T_g) range and Crystallinity Degree (X_c) of the PAEK matrix of welded specimens with six different interlayer forms.

Interlayer Forms	**T_g Range (°C)**	**Crystallinity (%)**
IF-1 (HE1-IG1)	137-161	26.92 ± 0.85
IF-2 (HE1-IG2)	139-160	24.13 ± 3.58
IF-3 (HE1-IG3)	141-163	24.13 ± 4.74
IF-4 (HE2-IG1)	138-158	27.37 ± 2.41
IF-5 (HE2-IG2)	139-162	25.74 ± 3.10
IF-6 (HE2-IG3)	138-161	26.63 ± 5.18

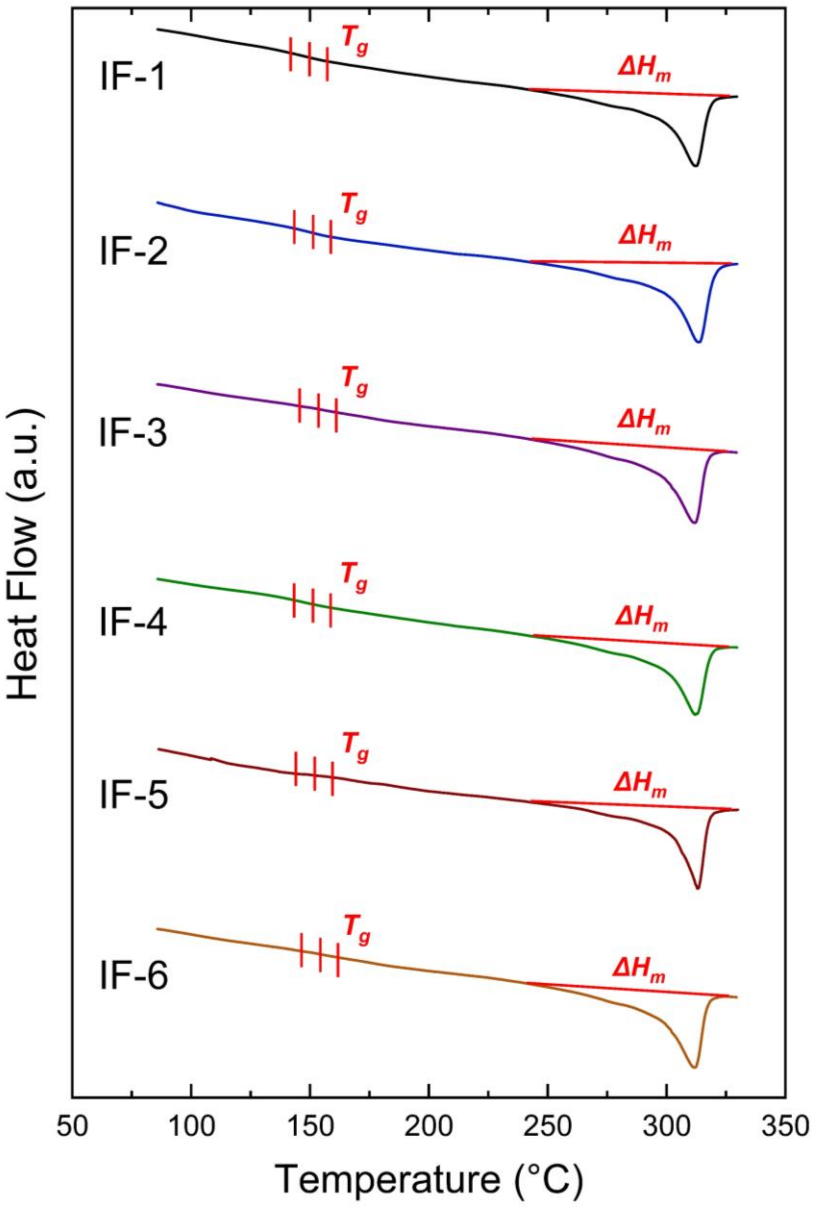

Figure 3.13 Examples of the first heating DSC thermograms of the welded specimens with six different Interlayer Forms.

Thus, it can be stated that, resistance welding parameters determined for the welding of PAEK/CF laminates with six different interlayer forms had no detrimental effects on the thermal behavior of the PAEK matrix. That is, temperature-time profiles applied for different specimens resulted in similar T_g ranges and allowed sufficient time necessary for the expected matrix crystallinity degree.

3.8 Comparison of the Welding Performance with Other Studies

As discussed in the Literature Review section, no reported research was found on the resistance welding of PAEK/CF composite laminates; thus it was not possible to compare welding performance obtained in this study with the other PAEK/CF studies.

In the literature, resistance welding studies on the Carbon Fiber reinforced composite laminates were conducted having other thermoplastic matrices, such as poly(etheretherketone) (PEEK) [29, 30, 31, 32, 36], poly(etherimide) (PEI) [28, 34, 37], poly(phenylenesulfide) (PPS) [27], etc. These studies used different Heating Elements and Insulating Layers in their Interlayer Forms. However, only limited number of studies [29, 30, 34, 36, 37] conducted mechanical tests to observe welding performance of their systems.

Therefore, in order to get an idea about the resistance welding performance of this study compared to other reported studies on the carbon fiber reinforced composite laminates with other thermoplastic matrices (PEEK and PEI), interlaminar shear strength (SLSS) values and interlaminar fracture toughness (G_{IC}) values obtained were compared in Table 3.6.

It was seen that, interlaminar mechanical properties obtained in this study for PAEK/CF laminates with IF-1 interlayer form were all above the values obtained in the other studies conducted for PEEK/CF and PEI/CF laminates.

This could be interpreted that resistance welding parameters used for the PAEK/CF specimens with IF-1 Interlayer Form might be considered as the basic proper start for further studies with more welding performance.

Table 3.6 Comparison of the mechanical properties obtained in the resistance welding of this study for PAEK/CF laminates with IF-1 interlayer form and the other studies conducted for PEEK/CF and PEI/CF laminates.

Studies	**Matrix / Reinforcement of the Laminate**	**SLSS (MPa)**	G_{IC} **(kJ/m^2)**
This study	PAEK/CF	36.77	3.76
Reference [29]	PEEK/CF	33.90	-
Reference [30]	PEEK/CF	-	1.90
Reference [36]	PEEK/CF	10 - 30	0.41 - 1.34
Reference [34]	PEI/CF	34.46	3.00 - 3.60
Reference [37]	PEI/CF	19.60	-

CHAPTER 4

CONCLUSIONS

Main conclusions drawn from the resistance welding studies of PAEK/CF thermoplastic composite laminates can be summarized as follows.

- Temperature-time profile studies indicated that during welding consolidation, for the homogenous melting and proper crystallization of the PAEK matrix, their dwell times should be 20 sec and 90 sec, respectively; under the power level of 50 V and pressure level of 6 bars. Then, for the six different Interlayer Forms, optimum "amperage" levels should be determined for the heating, melting and crystallization stages separately.

- After welding operations, Automated Ultrasonic Through Transmission inspection revealed that IF-1 and IF-4 Interlayer Forms with IG1 Insulating Glass Fiber layer had rather uniform color C-Scan mapping while the other Interlayer Forms with IG2 and IG3 insulating layers had C-Scan maps with certain degree of suspicious areas having sound wave attenuations (decibel losses).

- Mechanical tests indicated that welded specimens with IF-1 and IF-4 interlayer forms had the highest level of mechanical performance in terms of G_{IC} and G_{IIC} Interlaminar Fracture Toughness and SLSS Interlaminar Shear Strength.

- The only difference between IF-1 and IF-4 interlayer forms is their "Heating Element" layers designated as HE1 and HE2. Both of them are made of "Stainless Steel Meshes", having certain differences in terms of "Mesh Style" and "Areal Weight". Since both of them resulted in higher level of mechanical performance, it could be stated that use of these two different Stainless Steel Mesh forms as Heating Element layers, could be considered as an appropriate choice in the resistance welding of PAEK/CF laminates.

- The common layer in IF-1 and IF-4 interlayer forms was their "Insulating Layer" designated as IG1, which is actually a "Woven Glass Fiber" layer. Thus, it could be interpreted that the main reason of having very high-level mechanical performance in the welded specimens with IF-1 and IF-4 interlayer forms should be due to their IG1 insulating layer.

- Although IG1, IG2, IG3 insulating layers are all made of woven E-glass fibers, the differences are their "Fiber Diameter" and "Areal Weight", in which IG1 has much higher values. This means that during resistance welding operations, use of thicker and heavier Woven Glass Fiber insulating layers would perform their functions much more properly and efficiently.

- During resistance welding the main function of the "Insulating Layer" present in the "Interlayer Form" was to prevent "Current Leakage" to the other layers in the composite laminate. If current leakage occurs to the upper or lower composite laminates during welding, then not only voids could form in the thermoplastic matrix, but also delamination might occur in the upper or lower composite laminates being welded.

- Interlaminar failure mode observations during mechanical tests revealed that four typical modes (cohesive, adhesive, delamination and mixed) might take place depending on the weld performance. Cohesive Failure which represents higher quality of the welding operation, was especially observed in the specimens having IF-1 and IF-4 interlayer forms.

- Microscopic analyses proved that Thickness Deviation in all specimen groups after welding was all in an acceptable range while specimens with IF-1 and IF-4 interlayer forms after welding had the lowest Porosity Level.

- For all specimen groups DSC analyses showed that Glass Transition Temperature (T_g) range and Crystallinity Degree (X_c) of their PAEK matrix were the same after welding operations. Thus, it can be stated that, resistance welding parameters used had no detrimental effects on the thermal behavior of the PAEK matrix.

- Compared to the other reported studies on the resistance welding of carbon fiber reinforced composite laminates with other thermoplastic matrices (PEEK and PEI), it was observed that interlaminar mechanical properties obtained in this study for PAEK/CF laminates with IF-1 interlayer form were all above the values obtained for PEEK/CF and PEI/CF laminates.

As the final remark, it could be concluded that, resistance welding parameters used for the PAEK/CF specimens with IF-1 Interlayer Form might be considered as the basic proper start for further studies with more welding performance.

REFERENCES

[1] Beland, S. (1990). *High performance thermoplastic resins and their composites*. William Andrew. Published in USA, New Jersey.

[2] Ageorges, C., & Ye, L. (2002). *Fusion bonding of polymer composites*. Springer Science & Business Media. Pressed in Great Britain.

[3] Stavrov, D., & Bersee, H. E. (2003). Thermal aspects in resistance welding of thermoplastic composites. *Heat Transfer Summer Conference, 36959*, 151–156. doi: 10.1115/HT2003-47222.

[4] Stavrov, D., & Bersee, H. E. N. (2005). Resistance welding of thermoplastic composites-an overview. *Composites Part A: Applied Science and Manufacturing*, *36*(1), 39–54. doi: 10.1016/j.compositesa.2004.06.030.

[5] Ning, H., Lu, N., Hassen, A. A., Chawla, K., Selim, M., & Pillay, S. (2019). A review of long fibre thermoplastic (LFT) composites [A review of long fibre-reinforced thermoplastic of long fibre thermoplastic (LFT) composites]. *International Materials Reviews*, *64*(1). doi: 10.1080/09506608.2019.1585004.

[6] Gardiner, G. (2006). Thermoplastic composites gain leading edge on the A380: Breakthrough manufacturing process produces lightweight, affordable glass-reinforced PPS J-nose on the worlds largest commercial aircraft wing. *High Performance Composites, 14*(2), 50.

[7] Mathijsen, D. (2016). Leading the way in thermoplastic composites. *Reinforced Plastics, 60*(6), 405–407. doi: 10.1016/j.repl.2015.08.067.

[8] Bhudolia, S. K., Gohel, G., Leong, K. F., & Barsotti Jr, R. J. (2020). Investigation on ultrasonic welding attributes of novel carbon/elium® composites. *Materials, 13*(5), 1117. doi: 10.3390/ma13051117.

[9] Villegas, I. F., & Bersee, H. E. (2010). Ultrasonic welding of advanced thermoplastic composites: An investigation on energy-directing surfaces. *Advances in Polymer Technology*, *29*(2), 112–121. doi: 10.1002/adv.20178.

[10] Bhudolia, S. K., Gohel, G., Leong, K. F., & Islam, A. (2020). Advances in ultrasonic welding of thermoplastic composites: A review. *Materials*, *13*(6), 1284. doi: 10.3390/ma13061284.

[11] Villegas, I. F. (2019). Ultrasonic welding of thermoplastic composites. *Frontiers in Materials*, *6*, 291. doi: 10.3389/fmats.2019.00291.

[12] Krüger, S., Wagner, G., & Eifler, D. (2004). Ultrasonic welding of metal/composite joints. *Advanced Engineering Materials*, *6*(3), 157–159. doi: 10.1002/adem.200300539.

[13] Wang, K., Shriver, D., Li, Y., Banu, M., Hu, S. J., Xiao, G., Arinez, J., & Fan, H.-T. (2017). Characterization of weld attributes in ultrasonic welding of short carbon fiber reinforced thermoplastic composites. *Journal of Manufacturing Processes*, *29*, 124–132. doi: 10.1016/j.jmapro.2017.07.024.

[14] Wang, Y., Rao, Z., Liao, S., & Wang, F. (2021). Ultrasonic welding of fiber reinforced thermoplastic composites: Current understanding and challenges. *Composites Part A: Applied Science and Manufacturing*, *149*, 106578. doi: 10.1016/j.compositesa.2021.106578.

[15] Levy, A., Le Corre, S., & Villegas, I. F. (2014). Modeling of the heating phenomena in ultrasonic welding of thermoplastic composites with flat energy directors. *Journal of Materials Processing Technology*, *214*(7), 1361–1371. doi: 10.1016/j.jmatprotec.2014.02.009.

[16] Harras, B., Cole, K. C., & Vu-Khanh, T. (1996). Optimization of the ultrasonic welding of PEEK-carbon composites. *Journal of Reinforced Plastics and Composites*, *15*(2), 174–182. doi: 10.1177/073168449601500203.

[17] Benatar, A., & Gutowski, T. G. (1989). Ultrasonic welding of PEEK graphite APC-2 composites. *Polymer Engineering & Science*, *29*(23), 1705–1721. doi: 10.1002/pen.760292313.

[18] Barazanchy, D., & van Tooren, M. (2021). Heating mechanisms in induction welding of thermoplastic composites. *Journal of Thermoplastic Composite Materials*, 08927057211011621. doi: 10.1177/08927057211011621.

[19] Ahmed, T. J., Stavrov, D., Bersee, H. E. N., & Beukers, A. (2006). Induction welding of thermoplastic composites—An overview. *Composites Part A: Applied Science and Manufacturing*, *37*(10), 1638–1651. doi: 10.1016/j.compositesa.2005.10.009.

[20] Banik, N. (2018). A review on the use of thermoplastic composites and their effects in induction welding method. *Materials Today: Proceedings*, *5*(9), 20239–20249. doi: 10.1016/j.matpr.2018.06.395.

[21] Velmurugan, P., Manohar, J., Kannan, C. R., Manivannan, S., Vairamuthu, J., & Stalin, B. (2020). A study on development of induction welding of thermoplastic composites. *IOP Conference Series: Materials Science and Engineering*, *988*(1), 012109. doi: 10.1088/1757-899X/988/1/012109.

[22] Moser, L. (2012). *Experimental analysis and modeling of susceptorless induction welding of high performance thermoplastic polymer composites*.

[23] Schieler, O., & Beier, U. (2016). Induction welding of hybrid thermoplastic-thermoset composite parts. *Applied Science and Engineering Progress*, *9*(1), 27–36. doi: 10.14416/j.ijast.2015.10.005.

[24] Lionetto, F., Pappadà, S., Buccoliero, G., & Maffezzoli, A. (2017). Finite element modeling of continuous induction welding of thermoplastic matrix composites. *Materials & Design*, *120*, 212–221. doi: 10.1016/j.matdes.2017.02.024.

[25] Gouin O'Shaughnessey, P., Dube, M., & Fernandez Villegas, I. (2016). Modeling and experimental investigation of induction welding of thermoplastic composites and comparison with other welding processes. *Journal of Composite Materials*, *50*(21), 2895–2910. doi: 10.1177/0021998315614991.

[26] Farahani, R. D., & Dubé, M. (2017). Novel heating elements for induction welding of carbon fiber/polyphenylene sulfide thermoplastic composites. *Advanced Engineering Materials*, *19*(11), 1700294. doi: 10.1002/adem.201700294.

[27] Villegas, I. F., Moser, L., Yousefpour, A., Mitschang, P., & Bersee, H. E. (2013). Process and performance evaluation of ultrasonic, induction and resistance welding of advanced thermoplastic composites. *Journal of Thermoplastic Composite Materials*, *26*(8), 1007–1024. doi: 10.1177/0892705712456031.

[28] Ageorges, C., Ye, L., & Hou, M. (2000a). Experimental investigation of the resistance welding for thermoplastic-matrix composites. Part I: Heating element and heat transfer. *Composites Science and Technology*, *60*(7), 1027–1039. doi: 10.1016/S0266-3538(00)00005-1.

[29] Xiao, X. R., Hoa, S. V., & Street, K. N. (1992). Processing and modelling of resistance welding of APC-2 composite. *Journal of Composite Materials*, *26*(7), 1031–1049. doi: 10.1177/002199839202600705.

[30] Jakobsen, T. B., Don, R. C., & Gillespie Jr, J. W. (1989). Two-Dimensional thermal analysis of resistance welded thermoplastic composites. *Polymer Engineering & Science*, *29*(23), 1722–1729. doi: 10.1002/pen.760292314.

[31] Colak, Z. S., Sonmez, F. O., & Kalenderoglu, V. (2002). Process modeling and optimization of resistance welding for thermoplastic composites. *Journal of Composite Materials*, *36*(6), 721–744. doi: 10.1177/0021998302036006507.

[32] Holmes, S. T., & Gillespie Jr, J. W. (1993). Thermal analysis for resistance welding of large-scale thermoplastic composite joints. *Journal of Reinforced Plastics and Composites*, *12*(6), 723–736. doi: 10.1177/073168449301200609.

[33] Hou, M., & Friedrich, K. (1992). Resistance welding of continuous glass fibre-reinforced polypropylene composites. *Composites Manufacturing*, *3*(3), 153–163. doi: 10.1016/0956-7143(92)90078-9.

[34] Hou, M., Yang, M., Beehag, A., Mai, Y.-W., & Ye, L. (1999). Resistance welding of carbon fibre reinforced thermoplastic composite using alternative heating element. *Composite Structures*, *47*(1–4), 667–672. doi: 10.1016/S0263-8223(00)00047-7.

[35] Howie, I., Gillespie Jr, J. W., & Smiley, A. J. (1993). Resistance welding of graphite-polyarylsulfone/polysulfone dual-polymer composites. *Journal of Thermoplastic Composite Materials*, *6*(3), 205–225. doi: 10.1177/089270579300600303.

[36] Don, R. C., Gillespie Jr, J. W., & Lambing, C. L. (1992). Experimental characterization of processing-performance relationships of resistance welded graphite/polyetheretherketone composite joints. *Polymer Engineering & Science*, *32*(9), 620–631. doi: 10.1002/pen.760320908.

[37] Brassard, D., Dubé, M., & Tavares, J. R. (2019). Resistance welding of thermoplastic composites with a nanocomposite heating element. *Composites Part B: Engineering*, *165*, 779–784. doi: 10.1016/j.compositesb.2019.02.038.

[38] American Society for Testing and Materials, “Standard Test Methods for Constituent Content of Composite Materials 1,” 2015, doi: 10.1520/D3171-15.